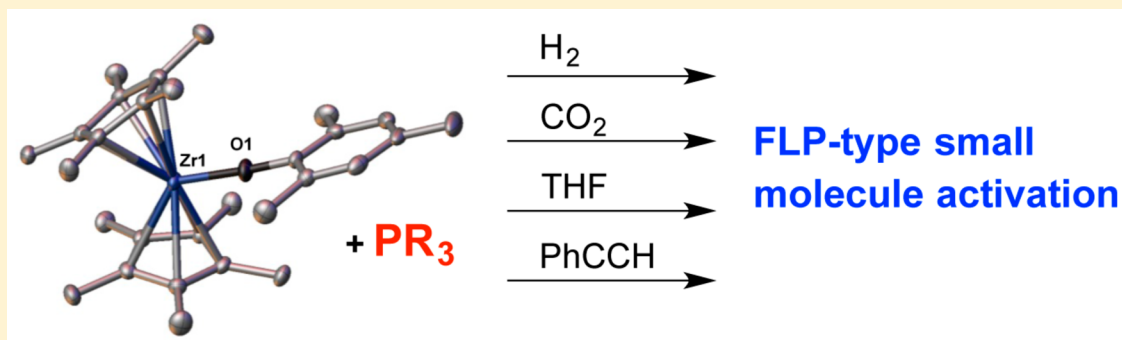


# Small Molecule Activation by Intermolecular Zr(IV)-Phosphine Frustrated Lewis Pairs

Owen J. Metters, Sebastian J. K. Forrest, Hazel A. Sparkes, Ian Manners, and Duncan F. Wass\*

School of Chemistry, University of Bristol, Cantock's Close, Bristol BS8 1TS, United Kingdom

**S** Supporting Information



**ABSTRACT:** We report intermolecular transition metal frustrated Lewis pairs (FLPs) based on zirconocene aryloxide and phosphine moieties that exhibit a broad range of small molecule activation chemistry that has previously been the preserve of only intramolecular pairs. Reactions with  $D_2$ ,  $CO_2$ , THF, and PhCCH are reported. By contrast with previous intramolecular examples, these systems allow facile access to a variety of steric and electronic characteristics at the Lewis acidic and Lewis basic components, with the three-step syntheses of 10 new intermolecular transition metal FLPs being reported. Systematic variation to the phosphine Lewis base is used to unravel steric considerations, with the surprising conclusion that phosphines with relatively small Tolman steric parameters not only give highly reactive FLPs but are often seen to have the highest selectivity for the desired product. DOSY NMR spectroscopic studies on these systems reveal for the first time the nature of the Lewis acid/Lewis base interactions in transition metal FLPs of this type.

## 1. INTRODUCTION

Frustrated Lewis pairs (FLPs) have proved to be a powerful new concept in small molecule activation and catalysis. By controlling the steric and electronic architecture of certain combinations of Lewis acids and bases to preclude the formation of a classical Lewis adduct, a high latent reactivity is imparted on the system.<sup>1</sup> This donor–acceptor ability is reminiscent of transition metal chemistry, and the ability of main group FLP systems to mimic reactivity normally associated with transition metals has been one of the remarkable features of this area. Initial investigations focused on the use of phosphine–borane FLPs and their ability to heterolytically cleave dihydrogen and facilitate hydrogenation reactions,<sup>2</sup> in addition to the binding and activation of carbon dioxide ( $CO_2$ ).<sup>3</sup> Subsequently, it was shown that main group FLPs are also able to mediate a wider range of transformations, such as 1,2-addition to alkynes<sup>4</sup> and the ring opening of cyclic ethers.<sup>5</sup>

A wide selection of inter- and intramolecular main group FLPs based on diverse Lewis acid and base groups has now been reported.<sup>6–8</sup> These pairs are able to mediate the heterolytic cleavage of  $H_2$ ,  $CO_2$  and isocyanate sequestration and deprotonation or 1,2 addition to terminal alkynes. Recent reports have also shown the utility of main group FLPs in

catalytic hydrogenation reactions. Intermolecular main group FLP systems are ubiquitous despite the obvious entropic disadvantages of this approach.

We, and others, have extended FLP chemistry to transition metals in the hope that combining the powerful small molecule activation chemistry of FLPs with the well-known suite of catalytically relevant reactions of transition metals could lead to yet more new chemistry.<sup>9</sup> Much of our initial focus has been on intramolecular systems in which the fluorinated borane fragment is replaced by an electrophilic group 4 metallocene (Figure 1, A–C). The chemistry of these cationic zirconocene–phosphinoaryloxide complexes in general mirrors main group systems (activation of  $H_2$ ,  $CO_2$ , THF), but also demonstrates reactivity that is either unique or rarely observed in main group systems, such as C–Cl and C–F bond cleavage, and catalytic dehydrocoupling of amine-boranes.<sup>10</sup> Other related intramolecular zirconocene-phosphine systems have also been reported by Erker et al. (Figure 1, D and E). These compounds are accessed through 1,1- or 1,2-carbozirconation reactions of alkynes to the zirconium(IV) cation  $[Cp^*_2ZrCH_3][B(C_6F_5)_4]$ . As with our intramolecular systems, these Zr/P pairs react with

Received: December 3, 2015

Published: January 20, 2016

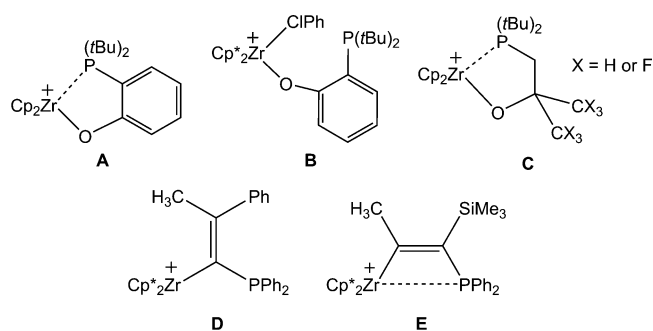
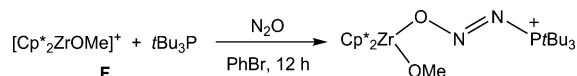


**Figure 1.** Intramolecular Zr/P FLPs developed by our group (A–C) and Erker et al. (D, E). In all cases, the  $[\text{B}(\text{C}_6\text{F}_5)_4]^-$  counterion is omitted for clarity.

a multitude of small molecules ( $\text{CO}$ ,  $\text{CO}_2$ ,  $\text{H}_2$ ,  $\text{N}_2\text{O}$ ,  $\text{PhC}(\text{H})\text{O}$ ,  $t\text{BuN}=\text{C}=\text{O}$ ,  $\text{N}_3-\text{Mes}$ , and  $\text{PhN}=\text{S}=\text{O}$ ).<sup>12</sup>

In stark contrast to the wide, varied and selective reactivity of these intramolecular FLPs, transformations mediated by intermolecular Zr/P FLPs are extremely limited. There are only two examples reported to date with the substrates employed limited to relatively reactive molecules containing highly polarized  $\text{C}=\text{O}$  or  $\text{N}-\text{O}$  bonds (example in Scheme 1).<sup>13</sup> This very narrow reactivity is doubly disappointing in that

### Scheme 1. Reactivity of an Intermolecular Zr/P FLP with $\text{N}_2\text{O}$



intermolecular systems offer the potential for more facile fine-tuning of electronic and steric parameters, for example, by using the wide range of commercially available phosphines, compared to the synthetically more challenging intramolecular analogues.

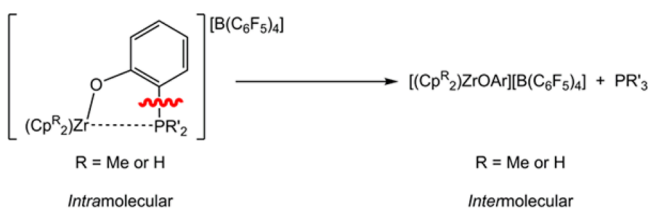
Certainly, an intermolecular system faces a more severe entropic challenge compared to its intramolecular analogue in bringing together three molecules. But the literature concerning main group FLPs is dominated by intermolecular systems, suggesting this should not be a fundamental impasse. Removal of the 1,2-aryl tether in our existing complexes (A–C) is an obvious way to design an intermolecular zirconocene aryloxy–phosphine FLP which could unlock this greater freedom in terms of tuning the steric and electronic properties of both the Lewis acidic electrophilic transition metal center and Lewis base (Scheme 2).

## 2. RESULTS AND DISCUSSION

### 2.1. Synthesis of Cationic Zirconocene Aryloxy Lewis Acids.

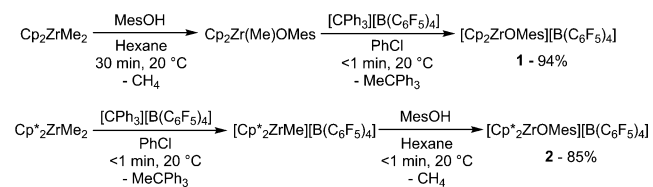
The required cationic Zr(IV) fragments shown in Scheme 2 were synthesized via two routes. The complex

### Scheme 2. Removal of the Aryl Tether to Give an Intermolecular FLP



bearing Cp ligands was accessed through preparation of  $[\text{Cp}_2\text{Zr}(\text{Me})\text{OMes}]$  ( $-\text{OMes} = 2,4,6\text{-trimethylphenoxide}$ ) by a modified literature procedure.<sup>14</sup> Subsequent methyl abstraction using  $[\text{CPh}_3][\text{B}(\text{C}_6\text{F}_5)_4]$  in a noncoordinating (PhCl) solvent gave  $[\text{Cp}_2\text{ZrOMes}][\text{B}(\text{C}_6\text{F}_5)_4]$  (**1**) in 94% yield. The Cp\* analogue was synthesized by an alternative route, as protonolysis of a methyl group from  $\text{Cp}^*_2\text{ZrMe}_2$  by 2,4,6-trimethylphenol (MesOH) was found to be extremely sluggish (60% yield after >10 days, 20 °C, hexane).  $[\text{Cp}^*_2\text{ZrOMes}][\text{B}(\text{C}_6\text{F}_5)_4]$  (**2**) was therefore accessed by initial methyl abstraction from  $\text{Cp}^*_2\text{ZrMe}_2$  using  $[\text{CPh}_3][\text{B}(\text{C}_6\text{F}_5)_4]$  prior to protonolysis of the remaining methyl group using MesOH (Scheme 3). This modification afforded the desired complex in 85% yield over two steps in minutes.

### Scheme 3. Synthesis of Zr(IV) Cations 1 and 2<sup>a</sup>



<sup>a</sup>Isolated yields are shown where applicable.

The molecular structure of Zr(IV) cations **1** and **2** are shown in Figure 2. Complex **1** is stabilized by solvent coordination (chlorobenzene) in the solid state causing a slight bending of the Zr–O1–Mes bond angle (153.2(2)°). This is contrary to species **2**, which exhibits an essentially linear Zr1–O1–Mes angle (176.7(2)°) indicative of multiple Zr–O bonding. Solvent coordination in **2** is presumably precluded by the additional steric bulk afforded by the Cp\* ligand. In **2**, unlike in previously structurally characterized examples of cationic Zr–aryloxy complexes, there is no evidence of an agostic interaction between the *ortho*-alkyl group and the electron deficient zirconium.<sup>15</sup>

### 2.2. Reaction with Phosphines: Generation of Frustrated Lewis Pairs (FLPs).

Taking our inspiration from main group systems and our previous intramolecular examples, initial attempts to generate an FLP system from **1** and **2** were made by addition of the bulky phosphine  $\text{P}^t\text{Bu}_3$ . However, this always

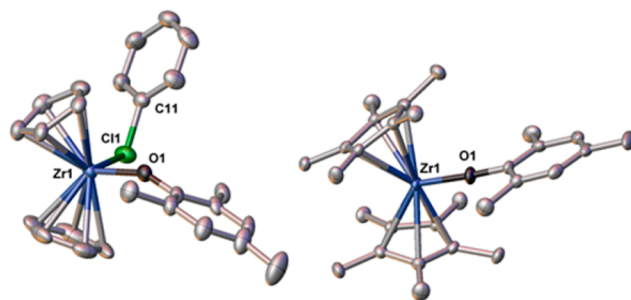


**Figure 2.** Molecular structure of **1** and **2** as determined by single crystal X-ray diffraction. Thermal ellipsoids are drawn at the 50% probability level. Hydrogens,  $[\text{B}(\text{C}_6\text{F}_5)_4]^-$  counterion, and PhCl solvent of crystallization are omitted for clarity. Selected bond lengths (Å) and angles (deg): **1**: Zr1–O1 1.935(2), Zr1–Cl1 2.6630(8), Zr1–Cl1–C11 120.7(1), Zr1–O1–Mes 153.2(2), Cp–Zr–Cp 130.2(6). **2**: Zr1–O1 1.937(2), O1–Mes 1.368(4), Zr1–O1–Mes 176.7(2), Cp\*–Zr–Cp\* 138.7(6).

resulted in an uncharacterizable mixture of products including appreciable amounts of  $[\text{HP}^t\text{Bu}_3][\text{B}(\text{C}_6\text{F}_5)_4]$  ( $^{31}\text{P}$  NMR  $\delta = 59.1$  ppm) which precluded further clean reactivity. By contrast, addition of an equimolar amount of a less basic and less sterically hindered phosphine ( $\text{PCy}_3$  (**a**),  $\text{PEt}_3$  (**b**),  $\text{PPh}_3$  (**c**),  $\text{PMes}_3$  (**d**), and  $\text{P}(\text{C}_6\text{F}_5)_3$  (**e**)) to **1** and **2** in chlorobenzene solution resulted in clean conversion to new species.

In this case  $^{31}\text{P}$  NMR spectroscopy is a useful probe for the nature of the Zr–P interaction, formation a Zr–P bond resulting in a large downfield shift (Table 1). In the case of **1**, it

**Table 1.**  $^{31}\text{P}$  NMR Chemical Shifts of Phosphines a–e and Lewis Pair Species 1a–e Correlated with the Relevant Tolman Steric Parameters ( $\theta$ )

$\text{PR}_3$	$^{31}\text{P}$ NMR, $\delta/\text{ppm}$	Zr/P	$^{31}\text{P}$ NMR, $\delta/\text{ppm}$	$\theta/^\circ$
$\text{PCy}_3$ ( <b>a</b> )	8.8	<b>1a</b>	23.8	170
$\text{PEt}_3$ ( <b>b</b> )	−19.2	<b>1b</b>	8.1	132
$\text{PPh}_3$ ( <b>c</b> )	−5.0	<b>1c</b>	21.2	145
$\text{PMes}_3$ ( <b>d</b> )	−36.5	<b>1d</b>	−36.5	212
$\text{P}(\text{C}_6\text{F}_5)_3$ ( <b>e</b> )	−75.5	<b>1e</b>	−75.5	184

was found that upon addition of  $\text{PCy}_3$ ,  $\text{PEt}_3$ , and  $\text{PPh}_3$ , a Zr–P interaction was formed with **1a**, **1b**, and **1c** all exhibiting large downfield shifts in their  $^{31}\text{P}$  NMR resonances, when compared to the free phosphine. The systems containing the more bulky  $\text{PMes}_3$  and  $\text{P}(\text{C}_6\text{F}_5)_3$ , **1d** and **1e**, show no change in their  $^{31}\text{P}$  NMR chemical shift, suggestive of the absence of a Zr–P interaction. In contrast, none of the systems with the bulkier  $\text{Cp}^*$  complex **2** (**2a–e**) show evidence of a Zr–P interaction in solution. This pattern is in good agreement with the Tolman steric parameters of the phosphines as shown in Table 1,<sup>16</sup> only the less bulky phosphines (with the less bulky zirconocene **1**) possess a Zr–P interaction. The less basic nature of the fluoroaryl substituted phosphine is also likely to be an important electronic consideration.

A DOSY (Diffusion-Ordered Spectroscopy) NMR study was undertaken to detect potential secondary interactions present between the Lewis acid and Lewis base, but also to further explore the nature of the interaction present in **1a–c**. A similar study has been carried out on main group  $\text{PR}_3/\text{B}(\text{C}_6\text{F}_5)_3$  ( $\text{R} = ^t\text{Bu}$  and  $\text{Mes}$ ) FLPs confirming secondary interactions are present between the fluorines on the  $\text{B}(\text{C}_6\text{F}_5)_3$  and the protons on  $\text{PR}_3$ .<sup>17</sup> Our study shows that in **1a–c** the interaction observed by  $^{31}\text{P}$  NMR spectroscopy is in fact dynamic and not a persistent Zr–P bond. For example, under our conditions ( $0.06 \text{ mol dm}^{-3}$ ,  $d_5$ -PhBr),<sup>18</sup> **1** was found to possess a diffusion coefficient ( $D$ ) of  $6.0 \times 10^{-10} \text{ m}^2 \text{ s}^{-1}$  and for  $\text{PEt}_3$  (**b**) a value of  $D = 19.5 \times 10^{-10} \text{ m}^2 \text{ s}^{-1}$ . Upon combination of **1** with 1 equiv of  $\text{PEt}_3$  to form **1b**, the values of  $D$  obtained for the two components were found to be  $5.5 \times 10^{-10} \text{ m}^2 \text{ s}^{-1}$  (**1**) and  $7.3 \times 10^{-10} \text{ m}^2 \text{ s}^{-1}$  ( $\text{PEt}_3$ ). The smaller diffusion coefficients in both cases indicate an interaction in solution consistent with the  $^{31}\text{P}$  NMR spectrum, however if the interaction was a persistent Zr–P bond the values of  $D$  for the two components should be equal. The nature of the interaction is therefore dynamic, with the equilibrium positioned toward the “bound” pair. Similar observations were made in the case of **1a** and **1c** (data in the Supporting Information).

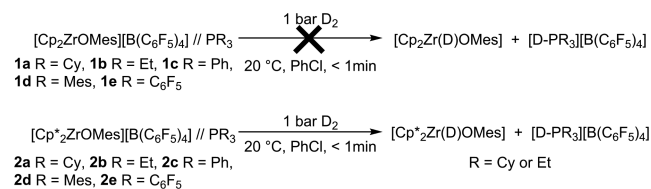
For FLP systems **1d–e** and **2a–e**, data obtained from DOSY experiments again shows the two components possessing smaller diffusion coefficients when in combination than when measured separately (Figures S15–S31). Taking **2b** as an

example, the values of  $D$  for the separate components are  $8.6 \times 10^{-10} \text{ m}^2 \text{ s}^{-1}$  (**2**) and  $19.5 \times 10^{-10} \text{ m}^2 \text{ s}^{-1}$  ( $\text{PEt}_3$ ), but upon combination these shift to  $8.0 \times 10^{-10} \text{ m}^2 \text{ s}^{-1}$  (**2**) and  $16.5 \times 10^{-10} \text{ m}^2 \text{ s}^{-1}$  ( $\text{PEt}_3$ , (**b**)). This suggests again that a dynamic equilibrium may be present with encounter complexes forming and separating in solution. In this case, however, the increased steric bulk of the  $\text{Cp}^*$  ligands means that a classical metal–phosphine bond cannot form; therefore, the dynamic equilibrium must arise from other weaker secondary interactions perhaps between the ancillary ligands. In conclusion, the DOSY study does indicate some degree of preorganization of the FLP prior to further reactions.

**2.3. Reactivity of Pairs with Dihydrogen ( $\text{D}_2$ ).** The heterolytic cleavage of  $\text{H}_2$  is perhaps the most typical example of small molecule activation mediated by FLPs and was a logical starting point here. For experimental expedience,  $\text{D}_2$  was used in place of  $\text{H}_2$  to allow more precise monitoring by  $^2\text{H}$  NMR spectroscopy.

When  $\text{PhCl}$  solutions of **1a–e** were pressurized with 1 bar  $\text{D}_2$  no reaction was observed (Scheme 4). This is consistent with

**Scheme 4.** Reactivity of FLP Systems **1a–e** and **2a–e** with 1 bar  $\text{D}_2$



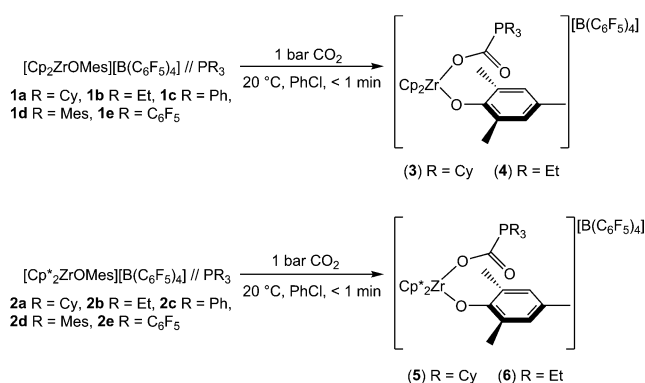
previous work where intramolecular Zr–P FLP systems bearing the  $\text{Cp}$  ligand set showed no reaction with  $\text{H}_2$  under similar conditions. Previous work has indicated the necessity for at least one  $\text{Cp}^*$  ligand to achieve heterolytic hydrogen cleavage, attributed to the more electron rich ligand facilitating transient binding of  $\text{H}_2$  to the Zr metal center and allowing deprotonation of this now more acidic species by the internal phosphine base. Consistent with this previous observation, **2a** and **2b** both showed an instantaneous reactions with 1 bar  $\text{D}_2$ . In the case of **2a**, a new species is observed by  $^{31}\text{P}$  NMR spectroscopy ( $\delta = 33.7$  ppm,  $^1J_{\text{PD}} = 67$  Hz) displaying a characteristic 1:1:1 splitting pattern indicative of the formation of a P–D bond. The  $^2\text{H}$  NMR spectrum confirms this assignment, with a doublet ( $\delta = 4.25$  ppm,  $^1J_{\text{PD}} = 67$  Hz) corresponding to the phosphonium deuteron and a sharp singlet ( $\delta = 5.96$  ppm) assigned as the Zr–deuteride. Treatment of **2b** with 1 bar  $\text{D}_2$  results in a similar downfield shift in the  $^{31}\text{P}$  NMR spectrum to give a 1:1:1 triplet again symptomatic of a P–D bond ( $\delta = 21.1$  ppm,  $^1J_{\text{PD}} = 67$  Hz). Species **2c–e** display no reactivity under the same conditions, with the lower basicity of these aryl-substituted phosphines being our working hypothesis for this observation.

In an attempt to probe the mechanism of the hydrogen cleavage reaction, a chlorobenzene solution of **2** was pressurized with  $\text{D}_2$  and cooled to  $-35$  °C, at which point no evidence for a Zr– $\text{D}_2$  complex was evident. These findings suggest a mechanism akin to that proposed by computational studies carried out on main-group FLP systems, in particular  $\text{P}^t\text{Bu}_3/\text{B}(\text{C}_6\text{F}_5)_3$ . In this case, it is proposed that preorganization of the FLP occurs prior to activation of the  $\text{H}_2$ . This is corroborated by our DOSY data discussed above which

indicates the presence of transient encounter complexes in solution.

**2.4. Reactivity of Pairs with Carbon Dioxide (CO<sub>2</sub>).** A range of main group and transition metal-based FLPs have shown the ability to sequester CO<sub>2</sub>.<sup>2,6–8</sup> The pairs **1a–e** and **2a–e** were treated with CO<sub>2</sub> by pressurizing chlorobenzene solutions of the species with 1 bar CO<sub>2</sub>. Upon pressurizing with CO<sub>2</sub>, systems **1a** and **1b** showed quantitative conversion to new species assigned as the CO<sub>2</sub> activation product by <sup>31</sup>P NMR spectroscopy (3  $\delta$  = 27.9 ppm, 4  $\delta$  = 28.0 ppm). Compound **1c** was found to yield two new species upon treatment with 1 bar CO<sub>2</sub> with <sup>31</sup>P NMR chemical shifts of 5.4 and 19.9 ppm, however the <sup>13</sup>C NMR spectrum showed no evidence of the carbonyl carbon. **1d** and **1e** were found to be inactive in the activation of CO<sub>2</sub> (Scheme 5).

**Scheme 5. Reactivity of FLP Systems 1a–e and 2a–e with 1 bar CO<sub>2</sub>**



**2a** and **2b** also react rapidly and quantitatively with 1 bar CO<sub>2</sub> giving rise to new species observed in the <sup>31</sup>P NMR spectrum at  $\delta$  = 24.9 ppm (**5**) and  $\delta$  = 24.1 ppm (**6**). As with **1c–e**, **2c** gives a mixture of products when treated with CO<sub>2</sub>, with no carbonyl peak visible in the <sup>13</sup>C NMR spectrum, and **2d** and **2e** display no reactivity (Scheme 5). It surprised us to some extent that the cleanest results were obtained with the relatively nonbulky alkyl phosphines **a** and **b**, even in the cases where a Zr–P interaction is observed (**1a** and **1b**); this echoes more recent results with main group FLPs where a truly “frustrated” system has been shown to be unnecessary so long as the Lewis acid and base can act in a cooperative fashion under the reaction conditions. The moniker “Cooperative Lewis Pairs” would seem to be increasingly appropriate. This also corroborates the DOSY study on **1a** and **1b**, which found that the Zr–P interaction is dynamic and a small amount of unbound Zr and PR<sub>3</sub> are present in solution. It is thought to be these species that react to form the desired products.

Crystallization under 1 bar CO<sub>2</sub> allows isolation of X-ray quality crystals of **6** in low (<5%) isolated yield.<sup>19</sup> The molecular structure of **6** is shown in Figure 3.

The solid state structure of **6** shows a slight lengthening of the Zr1–O2 bond length in comparison with **2** (1.962(2) Å vs 1.937(2) Å) indicative of a slight loss of the multiple bond character due to coordination of an additional ligand at the electron deficient Zr center. As expected, C30 appears to be tending toward sp<sup>2</sup> in character with values of 112.7(2)° and 117.8(2)° for the O3–C30–P1 and O2–C30–P1 angles, respectively, but a significantly larger angle (129.5(3)°) between O2–C30–O3 indicates that C30 retains some sp

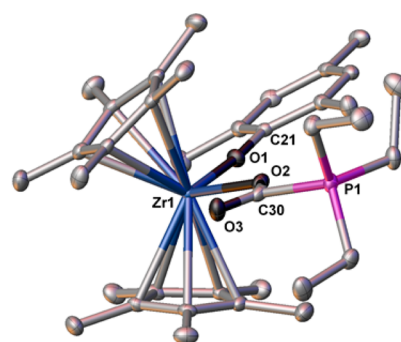
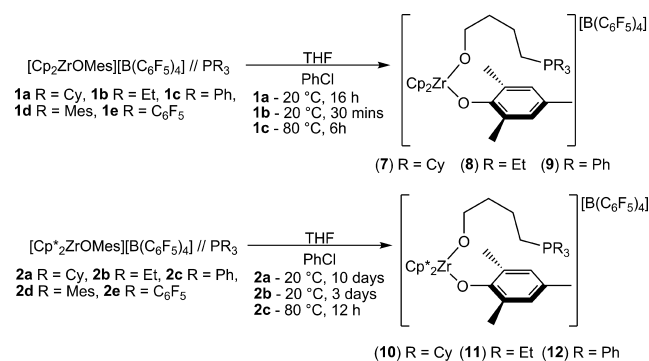


**Figure 3.** Molecular structure of **6** as determined by single crystal X-ray diffraction. Thermal ellipsoids are drawn at the 50% probability level. Hydrogens and the [B(C<sub>6</sub>F<sub>5</sub>)<sub>4</sub>]<sup>−</sup> counterion are omitted for clarity. Selected bond lengths (Å) and angles (deg): Zr1–O1 1.962(2), Zr1–O2 2.184(2), O2–C30 1.278(4), O3–C30 1.220(4), C30–P1 1.865(3), O2–C30–O3 129.5(3), O3–C30–P1 112.7(2), O2–C30–P1 117.8(2), Zr1–O1–C21 174.5(2), Zr1–O2–C30 129.1(2).

character. This is further reinforced by the only slightly longer C30–O2 bond length (1.278(4) Å) when compared to the C30–O3 double bond (1.220(4) Å).

**2.5. Reactivity of Pairs with Tetrahydrofuran (THF).** Treatment of chlorobenzene solutions of **1a–c** with an excess of THF results in an immediate color change from orange to yellow and concomitant dissociation of the bound phosphine to yield what is proposed to be [Cp<sub>2</sub>Zr(THF)OMes][B(C<sub>6</sub>F<sub>5</sub>)<sub>4</sub>]. **1a** reacts further to give quantitative conversion to **7** within 16h (<sup>31</sup>P NMR  $\delta$  = 38.4 ppm), **1b** undergoes a somewhat more rapid reaction to yield a species with a similar <sup>31</sup>P NMR shift (<sup>31</sup>P NMR  $\delta$  = 31.5 ppm) after 30 min assigned as **8**. **1c** shows no reaction at room temperature; however, upon heating to 80 °C for 6h full conversion to **9** is observed by <sup>31</sup>P NMR spectroscopy ( $\delta$  = 23.4 ppm). As with H<sub>2</sub> and CO<sub>2</sub>, **1d** and **1e** show no further reaction with THF despite heating at 80 °C for 16 h (Scheme 6).

**Scheme 6. Reactivity of FLP Systems 1a–e and 2a–e with THF**



To further probe the mechanism of this reaction, postulated intermediate [Cp<sub>2</sub>Zr(THF)OMes][B(C<sub>6</sub>F<sub>5</sub>)<sub>4</sub>] (1-THF) has been synthesized and isolated by reaction of **1** with THF, the molecular structure of which is shown in Figure 4.

In comparison to **1**, 1-THF shows a greater degree of bending of the Zr1–O1–Mes bond (139.8(8)° vs 153.2(2)°) in addition to a lengthening of the Zr1–O1 bond (1.972(1) Å vs 1.935(2) Å) due to the coordination of a more donating

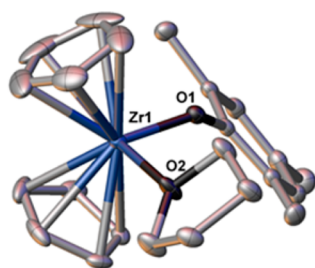


**Figure 4.** Molecular structures of **1-THF** as determined by single crystal X-ray diffraction. Thermal ellipsoids are drawn at the 50% probability level. Disorder around the THF ligand, hydrogens, and the  $[\text{B}(\text{C}_6\text{F}_5)_4]^-$  counterion are omitted for clarity. Selected bond lengths (Å) and angles (deg): Zr1–O1 1.972(1), Zr1–O2 2.206(1), Zr1–O1–Mes 139.8(8), O1–Zr1–O2 96.82(5).

ligand in the THF compared to chlorobenzene, thus further reducing the multiple bond character between the Zr and the aryloxide ligand.

Subsequent reaction of **1-THF** with  $\text{PR}_3$  (R = Cy, Et, Ph, Mes,  $\text{C}_6\text{F}_5$ ) results in reactivity identical to that shown in Scheme 6. We can therefore propose that the reaction mechanism consists of an initial complexation of THF to the Lewis acidic zirconocene center, which activates the THF toward nucleophilic attack at the  $\alpha$ -carbon by the phosphine. This mechanism fits well with the observed trend of the more nucleophilic phosphines giving more rapid reaction ( $\text{PEt}_3 > \text{PCy}_3 > \text{PPh}_3 > \text{PMes}_3 > \text{P}(\text{C}_6\text{F}_5)_3$ ). Reaction of **1-THF** with  $\text{PEt}_3$  being significantly more rapid than with  $\text{PCy}_3$  is thought to be a purely steric effect, with  $\text{PEt}_3$  having a cone angle of  $132^\circ$  compared to  $170^\circ$  for  $\text{PCy}_3$ . This mechanism is also consistent with works by Stephan et al. and Jordan et al., which describe the ring opening of Zr bound THF by phosphines and amines and independently conclude that the reaction proceeds by a Lewis acid activation of the C–O bond prior to nucleophilic attack at the  $\alpha$ -carbon.<sup>20</sup>

Similar, but overall less rapid reactivity is observed with **2a–e**. Upon addition of excess THF to chlorobenzene solutions of **2a–e** an immediate color change from red to yellow is observed indicating formation of a Zr–THF adduct as observed for **1a–e**. **2-THF** was isolated and characterized by the addition of THF to a chlorobenzene solution of **2**, and the molecular structure is shown in Figure 5. An interesting structural feature of **2-THF** is that, unlike its Cp analogue, the aryloxide ligand

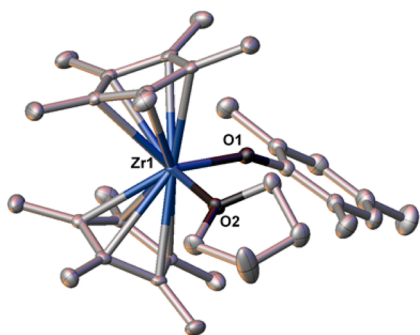


**Figure 5.** Molecular structure of **2-THF** as determined by single crystal X-ray diffraction. Hydrogens,  $[\text{B}(\text{C}_6\text{F}_5)_4]^-$  counterion, and solvent of crystallization are omitted for clarity. Selected bond lengths (Å) and angles (deg): Zr1–O1 1.984(1), Zr1–O2 2.282(1), O2–Zr1–O1 95.49(5), Zr1–O1–Mes 153.6(1).

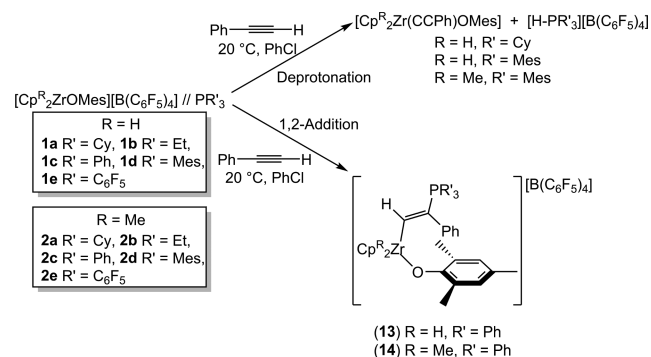
appears to be locked in conformation, with free rotation about the Zr1–O1–Mes axis precluded by the additional steric bulk. This is evidenced by the  $^1\text{H}$  NMR spectra for the two species, wherein **1-THF** is seen to possess two equivalent *ortho*- $\text{CH}_3$  groups ( $\delta = 1.84$  ppm (broad)); however, in **2-THF**, these become inequivalent ( $\delta = 1.79$  and  $1.88$  ppm).

The solid-state structure of **2-THF** also shows a significant bending of the Zr1–O1–Mes bond when compared to **2** ( $153.6(1)^\circ$  vs  $176.7(2)^\circ$ ). This is accompanied by an extension of the Zr1–O1 bond upon binding of THF (1.937(2) to 1.984(1) Å) again indicating that binding of an additional donor ligand to the Zr center reduces the multiple bond character of the Zr1–O1 bond.

Analogous to compound **1a**, species **2a** reacts with an excess of THF at room temperature to yield **10** in 10 days ( $^{31}\text{P}$  NMR  $\delta = 36.8$  ppm). Compound **2b** again reacts significantly faster, proceeding to a >99% conversion to **11** in 3 days ( $^{31}\text{P}$  NMR  $\delta = 30.2$  ppm). Compound **2c** shows no reactivity with THF at room temperature, but upon heating to  $80^\circ\text{C}$  complete conversion to **12** is observed within 12 h ( $^{31}\text{P}$  NMR  $\delta = 21.9$  ppm). As with the system bearing the Cp ligand set, the analogous Cp\* species **2d** and **2e** show no reaction with THF even at elevated temperature ( $80^\circ\text{C}$ , 24h). This general trend of the ring opening of cyclic ethers proceeding less rapidly with **2a–e** than **1a–e** is proposed to be a steric effect with Cp\* hindering the attack of the incoming phosphine nucleophile.

**2.6. Reactivity of Pairs with Alkynes.** The reaction of FLPs with terminal alkynes can proceed via one of two mechanisms, with the majority of main-group FLP systems going via a 1,2-addition reaction with the nature of the resulting isomer generally controlled by steric factors.<sup>4</sup> However, in previous work with Zr/P FLPs, it has been shown that a deprotonation reaction may also take place yielding a zirconium acetylide and phosphonium species (Scheme 7).<sup>11</sup>

#### Scheme 7. Reactivity of FLP Systems **1a–e** and **2a–e** with Phenylacetylene (PhCCH)



In the case of **1a**, upon addition of phenylacetylene (PhCCH), clean deprotonation is observed to yield  $[\text{HCy}_3]^-[\text{B}(\text{C}_6\text{F}_5)_4]^-$  ( $^{31}\text{P}$  NMR  $\delta = 33.1$  ppm,  $^1J_{\text{PH}} = 420$  Hz) and a zirconium acetylide complex. Surprisingly, compound **1b** shows a change in selectivity, and when treated with PhCCH it undergoes a slow reaction ( $20^\circ\text{C}$ , PhCl, 16 h) to yield a mixture of the two isomers of the 1,2-addition product (1:8). Separation of the isomers proved impossible due to their near identical solubility in a range of solvents. Reaction of **1c** with PhCCH rapidly ( $20^\circ\text{C}$ , PhCl, <1 min) yields the 1,2-addition product **13** ( $^{31}\text{P}\{^1\text{H}\}$  NMR  $\delta = 20.1$  ppm) with only the Zr/P *trans* isomer isolated. This was identified by comparison of the

$^1\text{H}$  NMR spectra to the crystallographically characterized analogue **14** vide infra. In both cases, the alkenyl proton exhibits a  $^3J_{\text{PH}}$  coupling of 45 Hz indicating an identical geometry around the double bond. A further change in selectivity is observed with **1d** with the favored reaction pathway reverting back to deprotonation, such that upon treatment of **1d** with PhCCH immediate formation of  $[\text{H-PMe}_3][\text{B}(\text{C}_6\text{F}_5)_4]$  is detected by  $^{31}\text{P}$  NMR spectroscopy ( $^{31}\text{P}$  NMR  $\delta = -27.5$  ppm,  $^1J_{\text{PH}} = 478$  Hz). Complex **1e** exhibits no reaction with PhCCH. The pairs **2a–e** exhibit a broadly similar trend in reactivity; however, both **2a** and **2b** yield a mixture of deprotonation and 1,2-addition products in ratios of 2:1 and 3:2, respectively. Again the system containing  $\text{PPh}_3$ , **2c**, reacts cleanly and rapidly with PhCCH to generate only the 1,2-addition product **14** ( $^{31}\text{P}\{^1\text{H}\}$  NMR  $\delta = 17.4$  ppm), the molecular structure of which is shown in Figure 6. As is observed with **1d** and **1e**, **2d** forms only the deprotonation product,  $[\text{H-PMe}_3][\text{B}(\text{C}_6\text{F}_5)_4]$ , and **2e** does not react upon addition of PhCCH.

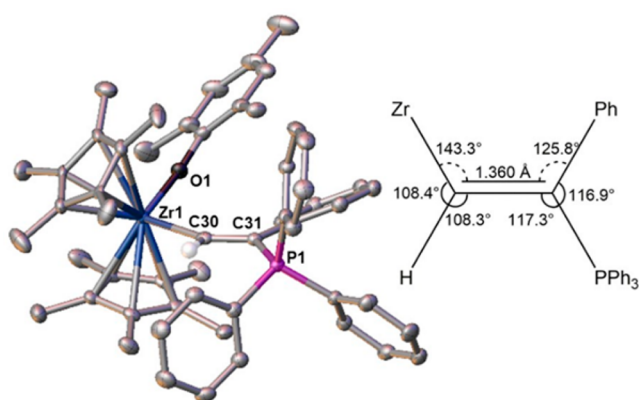


**Figure 6.** Molecular structure of **14** as determined by single crystal X-ray diffraction. Thermal ellipsoids are shown at the 50% probability level, and irrelevant hydrogens,  $[\text{B}(\text{C}_6\text{F}_5)_4]^-$  counterion, and disorder around the  $\text{Cp}^*$  rings are omitted for clarity. Inset is a representation of the  $\text{C}=\text{C}$  bond geometry. Selected bond lengths ( $\text{\AA}$ ) and angles (deg): Zr1–O1 1.971(2), Zr1–C30 2.327(3), C30–C31 1.360(3), P1–C31 1.815(3), O1–Zr1–C30 100.29(8), Zr1–O1–Mes 173.1(2), Zr1–C30–C31 143.3(2), C30–C31–Ph 125.8(2), Ph–C31–P1 116.9(2), P1–C31–C30 117.3(2).

The molecular structure of **14** (Figure 6) reveals the *trans*-Zr/P conformation with the Ph moiety of PhCCH geminal to  $\text{PPh}_3$ . This conformer is assumed to be preferred as it reduces steric clashes between the bulky  $\text{Cp}^*$  ligands with the phenyl rings of both  $\text{PPh}_3$  and PhCCH. C31 appears to possess a greater degree of  $\text{sp}^2$  character when compared to C30 as evidenced by the large Zr1–C30–C31 angle ( $143.3(2)^\circ$ ), this could again be attributed to the steric strain enforced by the interaction between the Ph group and the bulk aryloxy ligand on Zr.

These two competing reaction pathways have previously been observed by Erker et al., the main group FLP system  $\text{P}^t\text{Bu}_3/\text{B}(\text{C}_6\text{F}_5)_3$  reacting with a terminal alkyne to give the deprotonation product, whereas  $\text{PAr}_3/\text{B}(\text{C}_6\text{F}_5)_3$  ( $\text{PAr}_3 = \text{P}(o\text{-tolyl})_3$  or  $\text{P}\{\text{Ph}_2[2,5\text{-bis}(\text{trifluoromethyl})\text{phenyl}]\}$ ) cleanly yields the 1,2-addition product.<sup>4b</sup> This reactivity can generally be attributed to electronic factors with the more basic phosphines favoring deprotonation; however, there may also be a steric effect as  $\text{P}(o\text{-tolyl})_3$  and  $\text{PMe}_3$  are considered to be

electronically similar, but have significantly different steric parameters, with cone angles of  $194^\circ$  and  $212^\circ$ , respectively. This could be responsible for the switch in reactivity from 1,2-addition ( $\text{P}(o\text{-tolyl})_3$ , Erker et al.) to deprotonation ( $\text{PMe}_3$ , vide supra).

### 3. CONCLUSION

We have synthesized a range of intermolecular zirconium/phosphine FLPs derived from zirconocene cations and tertiary phosphines of varying steric and electronic properties. A DOSY NMR spectroscopic study on these systems has shown the nature of the Lewis acid/Lewis base interactions present in all cases. These pairs show for the first time the ability of intermolecular FLPs containing a transition metal fragment as the Lewis acid to react in an analogous fashion to their intramolecular counterparts.<sup>21</sup> These new systems are shown to mediate the activation of a range of small molecules ( $\text{D}_2$ ,  $\text{CO}_2$ , THF, phenylacetylene) with the reactivity toward these substrates highly dependent on the steric and electronic nature of the phosphine employed, a factor which had remained previously unexplored with transition metal FLPs. It has been found that the phosphine must be of sufficient basicity to promote such reactions; in all cases, systems using the weakly basic  $\text{P}(\text{C}_6\text{F}_5)_3$  (**1e** and **2e**) show no reactivity toward the small molecules studied. Given sufficient Lewis basicity, high steric bulk in the phosphine used is surprisingly unimportant; indeed, the least bulky phosphine used here,  $\text{PEt}_3$ , gives the cleanest results. In addition, the base used has a dramatic effect on selectivity, as evidenced by the switch in reaction mode with phenylacetylene from 1,2-addition to deprotonation when the less bulky  $\text{PPh}_3$  (**1c** and **2c**) is replaced with the significantly more bulky  $\text{PMe}_3$  (**1d** and **2d**). These results show that the use of intramolecular systems is not a prerequisite for transition metal FLPs and open many other possibilities for the design of intermolecular transition metal frustrated or cooperative Lewis pairs.

### 4. EXPERIMENTAL SECTION

**4.1. General Considerations.** Unless otherwise stated, all manipulations were undertaken under an atmosphere of argon or nitrogen using standard glovebox (M-Braun  $\text{O}_2 < 0.1$  ppm,  $\text{H}_2\text{O} < 0.1$  ppm) and Schlenk line techniques and all glassware were oven and vacuum-dried prior to use.  $\text{Cp}_2\text{ZrCl}_2$ ,  $\text{Cp}^*\text{ZrCl}_2\text{MeLi}$  (1.6 M in  $\text{Et}_2\text{O}$ ),  $\text{PCy}_3$ ,  $\text{PEt}_3$ ,  $\text{PPh}_3$ ,  $\text{PMe}_3$ , and  $\text{P}(\text{C}_6\text{F}_5)_3$  were purchased from Sigma-Aldrich and used as received.  $[\text{CPh}_3][\text{B}(\text{C}_6\text{F}_5)_4]$  was purchased from Acros Organics and used as received. 2,4,6-Trimethylphenol (MesOH) was purchased from Sigma-Aldrich and dried prior to use by stirring a hexane solution over  $\text{CaH}_2$  before removal of the solvent in vacuo and sublimation ( $25^\circ\text{C}$ ,  $2 \times 10^{-2}$  Torr). Phenylacetylene was purchased from Sigma-Aldrich and purified by distillation before use. Reagent gases ( $\text{D}_2$  and  $\text{CO}_2$ ) were dried prior to use by passing through a  $-78^\circ\text{C}$  trap.  $\text{Cp}_2\text{ZrMe}_2$  and  $\text{Cp}^*\text{ZrMe}_2$  were synthesized according to literature protocols.<sup>22</sup> Common laboratory solvents ( $\text{Et}_2\text{O}$ , DCM, hexane, THF) were purified using a Grubbs type purification system.<sup>23</sup> Nonstandard solvents (chlorobenzene, pentane) were purchased from Sigma-Aldrich and distilled from  $\text{CaH}_2$  prior to use.

NMR spectra were recorded using JEOL ECP-300 (300 MHz), Varian-400 (400 MHz), and Varian NMR500 (500 MHz) spectrometers. Deuterated solvents were obtained from Sigma-Aldrich ( $d_6$ -benzene,  $d_8$ -THF, and  $d_2$ -DCM) or Apollo Scientific ( $d_5$ -PhBr) and distilled from  $\text{CaH}_2$  prior to use. Spectra of air sensitive compounds were recorded using NMR tubes fitted with J. Young valves.

X-ray diffraction experiments were carried out at 100 K on a Bruker APEX II diffractometer using Mo  $K\alpha$  radiation ( $\lambda = 0.71073 \text{ \AA}$ ). For further details, see the Supporting Information.

Mass spectrometry experiments were carried out by the University of Bristol Mass Spectrometry Service on a Bruker Daltronics micrO TOF II with a TOF analyzer. All samples were run in predried PhCl.

**4.2. Synthesis of Zr Lewis acids.**  $Cp_2Zr(Me)OMes$ .  $Cp_2Zr(Me)OMes$  was prepared by a modified literature procedure.<sup>14</sup>  $Cp_2ZrMe_2$  (630 mg, 2.5 mmol) was dissolved in hexane (30 mL), and a solution of 2,4,6-trimethylphenol (323 mg, 2.5 mmol) in hexane (10 mL) was added dropwise. Effervescence was observed, and the resulting solution was stirred for 1 h. The solvent was removed in vacuo to yield a white solid. Recrystallization from hexanes at  $-78 \text{ }^\circ\text{C}$  gave a white crystalline solid (725 mg, 78%).

$^1\text{H}$  NMR (300 MHz,  $CD_2Cl_2$ )  $\delta$  0.31 (3H, s,  $CH_3$ ), 2.01 (6H, s, *ortho*- $CH_3$ ), 2.19 (3H, s, *para*- $CH_3$ ), 6.09 (10H, s, Cp), 6.73 (2H, s, aryl-H).

$[Cp_2ZrOMes][B(C_6F_5)_4]$  (**1**). In a glovebox, a chlorobenzene (1 mL) solution of  $[CPh_3][B(C_6F_5)_4]$  (198 mg, 0.2 mmol) was added dropwise to a stirred chlorobenzene (1 mL) solution of  $Cp_2Zr(Me)OMes$  (80 mg, 0.2 mmol). The orange solution was allowed to stir for 5 min before isolating the product via precipitation into a large volume (25 mL) of rapidly stirred hexane. The resulting yellow powder was washed with pentane ( $3 \times 5 \text{ mL}$ ) and dried in vacuo (204 mg, 94%).

$^1\text{H}$  NMR (300 MHz,  $C_6D_6$ )  $\delta$  1.74 (6H, s, *ortho*- $CH_3$ ), 2.19 (3H, s, *para*- $CH_3$ ), 5.49 (10H, s, Cp) 6.76 (2H, s, Ar-H).  $^{13}\text{C}$  NMR (125 MHz,  $C_6D_6$ )  $\delta$  17.1 (s, *ortho*- $CH_3$ ), 20.5 (s, *para*- $CH_3$ ), 117.5 (s, Cp), 128.77 (s, *ortho*-C), 130.0 (s, *meta*-C), 130.3 (s, *para*-C), 131.9 (s, *ipso*-C). ESI-MS (+ve detection) 355.0629  $m/z$   $[Cp_2ZrOMes]^+$ . Elem. Anal. Calcd (%): C, 49.87; H, 2.04. Found (%): C, 49.67; H, 2.63.

$[Cp^*ZrOMes][B(C_6F_5)_4]$  (**2**). In a glovebox, a chlorobenzene (1 mL) solution of  $[CPh_3][B(C_6F_5)_4]$  (94 mg, 0.1 mmol) was added dropwise to a stirred chlorobenzene solution of  $Cp^*ZrMe_2$  to give an orange solution. Upon dropwise addition of a chlorobenzene solution of 2,4,6-trimethylphenol (14 mg, 0.1 mmol), effervescence was observed accompanied by a color change from orange to deep red. After the effervescence had ceased (5 min), the product was isolated via precipitation into a large volume (25 mL) of rapidly stirred hexane. The resulting dark red powder was washed with pentane ( $3 \times 5 \text{ mL}$ ) and dried in vacuo (100 mg, 85%). Crystals of **2** suitable for analysis by single crystal X-ray diffraction were obtained by layering a chlorobenzene solution with pentane (3 days).

$^1\text{H}$  NMR (300 MHz,  $d_5$ -PhCl)  $\delta$  1.63 (30H, s,  $Cp^*$ ), 1.72 (6H, s, *ortho*- $CH_3$ ), 2.20 (3H, s, *para*- $CH_3$ ), 6.79 (2H, s, Ar-H).  $^{13}\text{C}$  NMR (125 MHz,  $d_5$ -PhCl)  $\delta$  13.9 (s,  $Cp^*$ - $CH_3$ ), 21.0 (s, *ortho*- $CH_3$ ), 23.6 (s, *para*- $CH_3$ ), 132.9 (s, Ar-CH), 137.1 (s, *ipso*-C). Other aryl carbons were obscured by PhCl peaks. ESI-MS (+ve detection) 495.2204  $m/z$   $[Cp^*ZrOMes]^+$ . Elem. Anal. Calcd (%): C, 54.14; H, 3.51. Found (%): C, 54.47; H, 3.80.

**4.3. Generation of FLPs.**  $[Cp_2ZrOMes][B(C_6F_5)_4] // PR_3$  (**1a–e**). In a glovebox, a chlorobenzene (0.5 mL) solution of **1** (30 mg, 0.029 mmol) was added to a chlorobenzene (0.5 mL) solution of  $PR_3$  (R = Cy (8.1 mg, 0.029 mmol), Et (3.4 mg, 0.029 mmol), Ph (7.6 mg, 0.029 mmol), Mes (11.3 mg, 0.029 mmol),  $C_6F_5$  (15.4 mg, 0.029 mmol)). Upon addition, a color change (orange to yellow) was observed for R = Cy, Et, and Ph, indicative of the presence of a Zr–P interaction.

For reaction of the FLP with substrates, the product was not isolated, but instead used in situ.

R = Cy.  $^{31}\text{P}$  NMR (121 MHz, PhCl)  $\delta$  24.3 (s, Zr- $PCy_3$ ). NB:  $PCy_3$   $\delta$  = 8.8.

R = Et.  $^{31}\text{P}$  NMR (121 MHz, PhCl)  $\delta$  8.1 (s, Zr- $PEt_3$ ). NB:  $PEt_3$   $\delta$  =  $-19.2$ .

R = Ph.  $^{31}\text{P}$  NMR (121 MHz, PhCl)  $\delta$  21.2 (s, Zr- $PPh_3$ ). NB:  $PPh_3$   $\delta$  =  $-5.0$ .

R = Mes.  $^{31}\text{P}$  NMR (121 MHz, PhCl)  $\delta$   $-36.5$  (s,  $PMes_3$ ). NB:  $PMes_3$   $\delta$  =  $-36.5$ .

R =  $C_6F_5$ .  $^{31}\text{P}$  NMR (121 MHz, PhCl)  $\delta$   $-75.5$  (s,  $P(C_6F_5)_3$ ). NB:  $P(C_6F_5)_3$   $\delta$  =  $-75.5$ .

$[Cp^*ZrOMes][B(C_6F_5)_4] // PR_3$  (**2a–e**). In a glovebox, a chlorobenzene (0.5 mL) solution of **2** (30 mg, 0.025 mmol) was

added to a chlorobenzene (0.5 mL) solution of  $PR_3$  (R = Cy (7.1 mg, 0.025 mmol), Et (3.0 mg, 0.025 mmol), Ph (6.7 mg, 0.025 mmol), Mes (9.9 mg, 0.025 mmol),  $C_6F_5$  (14.0 mg, 0.025 mmol)). Upon addition, no change in color of  $^{31}\text{P}$  NMR chemical shift was observed. For reaction of the FLP with substrates, the product was not isolated, but instead used in situ.

**4.4. DOSY Study of 1a–e and 2a–e.** Samples of **1a–e** and **2a–e** and separate control samples of **1**, **2**, and  $PR_3$  (R = Cy, Et, Ph, Mes,  $C_6F_5$ ) were made as detailed above, but dissolved in  $d_5$ -PhBr. In the case of **1**, **2**,  $PR_3$  (R = Cy, Et, Ph, Mes), **1a–d**, and **2a–d**,  $^1\text{H}$  DOSY NMR spectroscopy experiments were carried out using 15 increments and a diffusion delay of 100 ms. For **1e**, **2e**, and  $P(C_6F_5)_3$ , the analogous experiment was carried out using  $^{19}\text{F}$  DOSY NMR spectroscopy due to the lack of protons on the  $P(C_6F_5)_3$ . The results of the study can be found in Figures S15–S31: All data was analyzed using DOSY-Toolbox.<sup>24</sup>

**4.5. Reaction of Pairs with  $D_2$ .** Reactivity of  $[Cp_2ZrOMes][B(C_6F_5)_4]//PR_3$  (**1a–e**). In a glovebox, **1** (30 mg, 0.028 mmol) and an equimolar amount of the corresponding phosphine (0.028 mmol, **a** =  $PCy_3$  (8.1 mg), **b** =  $PEt_3$  (3.4 mg), **c** =  $PPh_3$  (7.6 mg), **d** =  $PMes_3$  (11.3 mg), **e** =  $P(C_6F_5)_3$  (15.4 mg)) were weighed out and dissolved in PhCl (0.7 mL) before transferring to an NMR tube fitted with a J. Young valve. Following removal from the glovebox, the sample was subjected to a freeze–pump–thaw degassing cycle prior to refilling with 1 bar  $D_2$ . In all cases, no change in the  $^{31}\text{P}$  NMR spectra was observed following addition of  $D_2$ .

Reactivity of  $[Cp^*ZrOMes][B(C_6F_5)_4]//PR_3$  (**2a–e**). In a glovebox, **2** (30 mg, 0.026 mmol) and an equimolar amount of the corresponding phosphine (0.026 mmol, **a** =  $PCy_3$  (7.1 mg), **b** =  $PEt_3$  (3.0 mg), **c** =  $PPh_3$  (6.7 mg), **d** =  $PMes_3$  (9.9 mg), **e** =  $P(C_6F_5)_3$  (14.0 mg)) were weighed out and dissolved in PhCl (0.7 mL) before transferring to an NMR tube fitted with a J. Young valve. Following removal from the glovebox, the sample was subjected to a freeze–pump–thaw degassing cycle prior to refilling with 1 bar  $D_2$ . In the case of **2a** and **2b**, an instantaneous color change from red to pale yellow was observed. Collected spectral data is detailed below:

**2a** +  $D_2$ .  $^{31}\text{P}$  NMR (121 MHz, PhCl)  $\delta$  33.6 (1:1:1 triplet,  $^1J_{PD}$  = 68 Hz,  $[DPCy_3]^+$ ).  $^2\text{H}$  NMR (46 MHz, PhCl)  $\delta$  4.22 (d,  $^1J_{PD}$  = 68 Hz,  $[DPCy_3]^+$ ), 5.98 (s, Zr-D).

**2b** +  $D_2$ .  $^{31}\text{P}$  NMR (121 MHz, PhCl)  $\delta$  21.2 (1:1:1 triplet,  $^1J_{PD}$  = 68 Hz,  $[DPEt_3]^+$ ).  $^2\text{H}$  NMR (46 MHz, PhCl)  $\delta$  4.40 (v. broad,  $[DPEt_3]^+$ ), 5.98 (s, Zr-D).

**4.6. Reaction of Pairs with  $CO_2$ .** Reactivity of  $[Cp_2ZrOMes][B(C_6F_5)_4]//PR_3$  (**1a–e**). In a glovebox, **1** (30 mg, 0.028 mmol) and an equimolar amount of the corresponding phosphine (0.028 mmol, **a** =  $PCy_3$  (8.1 mg), **b** =  $PEt_3$  (3.4 mg), **c** =  $PPh_3$  (7.6 mg), **d** =  $PMes_3$  (11.3 mg), **e** =  $P(C_6F_5)_3$  (15.4 mg)) were weighed out and dissolved in PhCl (0.7 mL) before transferring to an NMR tube fitted with a J. Young valve. Following removal from the glovebox, the sample was subjected to a freeze–pump–thaw degassing cycle prior to refilling with 1 bar  $CO_2$  via a  $-78 \text{ }^\circ\text{C}$  trap. In the cases of **1a**, **1b**, and **1c**, an immediate lightening of the yellow color was observed. In all cases, isolation under 1 bar  $CO_2$  was attempted, but was not possible. As such all spectral data was obtained in situ.

**Compound 3.**  $^1\text{H}$  NMR (500 MHz, PhCl)  $\delta$  1.60–1.81 (30H, m,  $PCy_3$ ), 1.99 (6H, s, *ortho*- $CH_3$ ), 2.20 (3H, s, *para*- $CH_3$ ), 6.13 (10H, s, Cp), 6.76 (2H, s, Ar-H).  $^{13}\text{C}$  NMR (125 MHz, PhCl)  $\delta$  17.7 (s, *ortho*- $CH_3$ ), 20.3 (s, *para*- $CH_3$ ), 25.2 (s, *para*-C ( $PCy_3$ )), 26.4 (d,  $^3J_{PC}$  = 12 Hz, *meta*-C ( $PCy_3$ )), 26.9 (d,  $^2J_{PC}$  = 4 Hz, *meta*-C ( $PCy_3$ )), 30.7 (d,  $^1J_{PC}$  = 33 Hz, *ipso*-C ( $PCy_3$ )), 114.7 (s, Cp), 123.3 (s, *para*-C), 124.6 (s, *ortho*-C), 160.4 (s, *ipso*-C), 162.5 (d,  $^1J_{PC}$  = 100 Hz, C(O)=O). NB: *meta*-C peak obscured by PhCl.  $^{31}\text{P}$  NMR (121 MHz, PhCl)  $\delta$  27.9 (s).

**Compound 4.**  $^1\text{H}$  NMR (500 MHz, PhCl)  $\delta$  0.97 (9H, t,  $CH_3$  ( $PEt_3$ )), 1.78 (6H, m,  $CH_2$  ( $PEt_3$ )), 1.93 (6H, s, *ortho*- $CH_3$ ), 2.21 (3H, s, *para*- $CH_3$ ), 6.09 (10H, s, Cp), 6.76 (2H, s, Ar-H).  $^{13}\text{C}$  NMR (125 MHz, PhCl)  $\delta$  5.3 (d,  $^2J_{PC}$  = 5 Hz), 11.4 (d,  $^1J_{PC}$  = 42 Hz), 17.3 (s, *ortho*- $CH_3$ ), 20.3 (s, *para*- $CH_3$ ), 114.9 (s, Cp), 123.3 (s, *para*-C), 124.6 (s, *ortho*-C), 160.3 (s, *ipso*-C), 162.4 (d,  $^1J_{PC}$  = 112 Hz, C(O)=

O). NB: *meta*-C peak obscured by PhCl.  $^{31}\text{P}$  NMR (121 MHz, PhCl)  $\delta$  27.6 (s).

**Reactivity of  $[\text{Cp}^*_2\text{ZrOMes}][\text{B}(\text{C}_6\text{F}_5)_4]/\text{PR}_3$  (**2a–e**).** In a glovebox, **2** (30 mg, 0.026 mmol) and an equimolar amount of the corresponding phosphine (0.026 mmol, **a** =  $\text{PCy}_3$  (7.1 mg), **b** =  $\text{PET}_3$  (3.0 mg), **c** =  $\text{PPh}_3$  (6.7 mg), **d** =  $\text{PMes}_3$  (9.9 mg), **e** =  $\text{P}(\text{C}_6\text{F}_5)_3$  (14 mg)) were weighed out and dissolved in PhCl (0.7 mL) before transferring to an NMR tube fitted with a J. Young valve. Following removal from the glovebox, the sample was subjected to a freeze–pump–thaw degassing cycle prior to refilling with 1 bar  $\text{CO}_2$  via a  $-78^\circ\text{C}$  trap. In the cases of **2a**, **2b**, and **2c**, an immediate color change from red to yellow was observed. In all cases, isolation under 1 bar  $\text{CO}_2$  was attempted, but was only possible in the case of **6** and in <5% yield. As such all spectral data was obtained *in situ*.

**Compound 5.**  $^1\text{H}$  NMR (500 MHz, PhCl)  $\delta$  1.02 (9H, m,  $\text{CH}_3$  ( $\text{PEt}_3$ )), 1.69 (30H, s,  $\text{Cp}^*$ ), 1.87 (6H, m,  $\text{CH}_2$  ( $\text{PEt}_3$ ), 1.94 (3H, s, *ortho*- $\text{CH}_3$ ), 2.00 (3H, s, *ortho*- $\text{CH}_3$ ), 2.19 (3H, s, *para*- $\text{CH}_3$ ), 6.67 (2H, s, Ar–H).  $^{13}\text{C}$  NMR (125 MHz, PhCl)  $\delta$  11.7 (s,  $\text{Cp}^*$ ), 18.7 and 19.8 (s, *ortho*- $\text{CH}_3$ ), 20.1 (s, *para*- $\text{CH}_3$ ), 25.1 (s, *para*-C ( $\text{PCy}_3$ )), 26.5 (d,  $^3J_{\text{PC}} = 12$  Hz, *meta*-C ( $\text{PCy}_3$ )), 27.2 (d,  $^2J_{\text{PC}} = 4$  Hz, *ortho*-C ( $\text{PCy}_3$ )), 32.0 (d,  $^1J_{\text{PC}} = 30$  Hz, *ipso*-C ( $\text{PCy}_3$ )), 122.6 (s,  $\text{Cp}^*$ ), 124.1 (s, *para*-C), 124.6 (s, *ortho*-C), 156.4 (s, *ipso*-C), 161.6 (d,  $^1J_{\text{PC}} = 92$  Hz,  $\text{C}(\text{O})=\text{O}$ ). NB: *meta*-C peak obscured by PhCl.  $^{31}\text{P}$  NMR (121 MHz, PhCl):  $\delta$  22.5 (s).

**Compound 6.**  $^1\text{H}$  NMR (500 MHz, PhCl)  $\delta$  1.02 (9H, m,  $\text{CH}_3$  ( $\text{PEt}_3$ )), 1.69 (30H, s,  $\text{Cp}^*$ ), 1.87 (6H, m,  $\text{CH}_2$  ( $\text{PEt}_3$ ), 1.94 (3H, s, *ortho*- $\text{CH}_3$ ), 2.00 (3H, s, *ortho*- $\text{CH}_3$ ), 2.19 (3H, s, *para*- $\text{CH}_3$ ), 6.67 (2H, s, Ar–H).  $^{13}\text{C}$  NMR (125 MHz, PhCl)  $\delta$  5.4 (d,  $^2J_{\text{PC}} = 5$  Hz), 11.3 (s,  $\text{Cp}^*$ ), 11.8 (d,  $^1J_{\text{PC}} = 42$  Hz), 18.1 and 19.6 (s, *ortho*- $\text{CH}_3$ ), 20.2 (s, *para*- $\text{CH}_3$ ), 122.4 (s,  $\text{Cp}^*$ ), 123.9 (s, *para*-C), 124.6 (s, *ortho*-C), 156.2 (s, *ipso*-C), 161.6 (d,  $^1J_{\text{PC}} = 108$  Hz,  $\text{C}(\text{O})=\text{O}$ ). NB: *meta*-C peak obscured by PhCl.  $^{31}\text{P}$  NMR (121 MHz, PhCl):  $\delta$  27.9 (s).

**4.7. Reaction of PhCl with THF. Reactivity of  $[\text{Cp}_2\text{ZrOMes}][\text{B}(\text{C}_6\text{F}_5)_4]/\text{PR}_3$  (**1a–e**).** In a glovebox, **1** (30 mg, 0.028 mmol) and an equimolar amount of the corresponding phosphine (0.019 mg, **a** =  $\text{PCy}_3$  (8.1 mg), **b** =  $\text{PET}_3$  (3.4 mg), **c** =  $\text{PPh}_3$  (7.6 mg), **d** =  $\text{PMes}_3$  (11.3 mg), **e** =  $\text{P}(\text{C}_6\text{F}_5)_3$  (15.4 mg)) were weighed out and dissolved in PhCl (0.7 mL) before transferring to an NMR tube fitted with a J. Young valve. The resulting solution was treated with five drops of THF, and a slight lightening of the yellow color observed. The  $^{31}\text{P}$  NMR spectrum of the solution indicated full conversion to free phosphine in all cases caused by its displacement by the THF moiety. When the reaction was deemed complete by  $^{31}\text{P}$  NMR spectroscopy, the product was isolated by precipitation into rapidly stirred hexane, washed with pentane ( $3 \times 5$  mL), and dried *in vacuo*.

**Compound 7.** Yield = 24 mg (60%).  $^1\text{H}$  NMR (500 MHz,  $d_8$ -THF)  $\delta$  1.80–2.04 (34H, m,  $\text{PCy}_3$ ,  $\beta$ - $\text{CH}_2$  and  $\gamma$ - $\text{CH}_2$ ), 2.10 (6H, s, *ortho*- $\text{CH}_3$ ), 2.21 (3H, s, *para*- $\text{CH}_3$ ), 2.28 (2H, m,  $\delta$ - $\text{CH}_2$ ), 4.12 (2H, t,  $^3J_{\text{HH}} = 6$  Hz,  $\alpha$ - $\text{CH}_2$ ), 6.23 (10H, s, Cp), 6.69 (2H, s, Ar–H).  $^{13}\text{C}$  NMR (125 MHz,  $d_8$ -THF)  $\delta$  16.3 (d,  $^1J_{\text{PC}} = 43$  Hz,  $\delta$ - $\text{CH}_2$ ), 18.2 (s, *ortho*- $\text{CH}_3$ ), 20.7 (d,  $^2J_{\text{PC}} = 5$  Hz,  $\gamma$ - $\text{CH}_2$ ), 20.8 (s, *para*- $\text{CH}_3$ ), 23.3 (s, *para*-C ( $\text{PCy}_3$ )), 27.5 (d,  $^3J_{\text{PC}} = 12$  Hz, *meta*-C ( $\text{PCy}_3$ )), 27.8 (d,  $^2J_{\text{PC}} = 4$  Hz, *ortho*-C ( $\text{PCy}_3$ )), 30.8 (d,  $^1J_{\text{PC}} = 42$  Hz, *ipso*-C ( $\text{PCy}_3$ )), 36.7 (d,  $^3J_{\text{PC}} = 14$  Hz,  $\beta$ - $\text{CH}_2$ ), 73.3 (s,  $\alpha$ - $\text{CH}_2$ ), 113.7 (s, Cp), 125.6 (s, *para*-C), 127.6 (s, *ortho*-C), 129.7 (s, *meta*-C), 162.0 (s, *ipso*-C).  $^{31}\text{P}$  NMR (121 MHz, PhCl)  $\delta$  31.5 (s). ESI-MS (+ve detection) 707.3522  $m/z$  [ $\text{M}]^+$ , 353.2962  $m/z$  [ $\text{HO}(\text{C}_4\text{H}_8)\text{PCy}_3]^+$ .

**Compound 8.** Yield = 23 mg (65%).  $^1\text{H}$  NMR (500 MHz,  $d_8$ -THF)  $\delta$  1.31 (9H, m,  $(\text{CH}_3)\text{PEt}_3$ ), 1.70 (2H, m,  $\beta$ - $\text{CH}_2$  and  $\gamma$ - $\text{CH}_2$ ), 2.09 (6H, s, *ortho*- $\text{CH}_3$ ), 2.21 (3H, s, *para*- $\text{CH}_3$ ), 2.24 (2H, m,  $\gamma$ - $\text{CH}_2$ ), 2.27 (6H, m,  $(\text{CH}_2)\text{PEt}_3$ ), 2.31 (2H, m,  $\delta$ - $\text{CH}_2$ ), 4.10 (2H, t,  $^3J_{\text{HH}} = 6$  Hz,  $\alpha$ - $\text{CH}_2$ ), 6.23 (10H, s, Cp), 6.69 (2H, s, Ar–H).  $^{13}\text{C}$  NMR (125 MHz,  $d_8$ -THF)  $\delta$  5.62 (d,  $^2J_{\text{PC}} = 5$  Hz,  $(\text{CH}_3)\text{PEt}_3$ ), 12.1 (d,  $^1J_{\text{PC}} = 49$  Hz,  $(\text{CH}_2)\text{PEt}_3$ ), 18.2 (s, *ortho*- $\text{CH}_3$ ), 18.9 (d,  $^1J_{\text{PC}} = 45$  Hz,  $\delta$ - $\text{CH}_2$ ), 19.3 (d,  $^2J_{\text{PC}} = 5$  Hz,  $\gamma$ - $\text{CH}_2$ ), 20.8 (s, *para*- $\text{CH}_3$ ), 36.2 (d,  $^3J_{\text{PC}} = 14$  Hz,  $\beta$ - $\text{CH}_2$ ), 73.3 (s,  $\alpha$ - $\text{CH}_2$ ), 113.7 (s, Cp), 125.6 (s, *para*-C), 127.6 (s, *ortho*-C), 129.7 (s, *meta*-C), 162.0 (s, *ipso*-C).  $^{31}\text{P}$  NMR (121 MHz, PhCl)  $\delta$  38.0 (s). ESI-MS (+ve detection) 545.2118  $m/z$  [ $\text{M}]^+$ , 191.1536  $m/z$  [ $\text{HO}(\text{C}_4\text{H}_8)\text{PEt}_3]^+$ .

**Compound 9.** Yield = 27 mg (68%).  $^1\text{H}$  NMR (500 MHz,  $d_8$ -THF)  $\delta$  1.74 (2H, m,  $\beta$ - $\text{CH}_2$ ), 1.83 (2H, m,  $\gamma$ - $\text{CH}_2$ ), 2.01 (6H, s, *ortho*- $\text{CH}_3$ ), 2.16 (3H, s, *para*- $\text{CH}_3$ ), 3.40 (2H, m,  $\delta$ - $\text{CH}_2$ ), 4.08 (2H, t,  $^3J_{\text{HH}} = 6$  Hz,  $\alpha$ - $\text{CH}_2$ ), 6.13 (10H, s, Cp), 6.67 (2H, s, Ar–H), 7.70–7.89 (15H, m,  $\text{PPh}_3$ ).  $^{13}\text{C}$  NMR (125 MHz,  $d_8$ -THF):  $\delta$  17.8 (s, *ortho*- $\text{CH}_3$ ), 20.4 (d,  $^2J_{\text{PC}} = 5$  Hz,  $\gamma$ - $\text{CH}_2$ ), 20.5 (s, *para*- $\text{CH}_3$ ), 22.6 (d,  $^1J_{\text{PC}} = 51$  Hz,  $\delta$ - $\text{CH}_2$ ), 35.7 (d,  $^3J_{\text{PC}} = 16$  Hz,  $\beta$ - $\text{CH}_2$ ), 72.7 (s,  $\alpha$ - $\text{CH}_2$ ), 113.3 (s, Cp), 119.3 (d,  $^1J_{\text{PC}} = 86$  Hz, *ipso*-C ( $\text{PPh}_3$ )), 125.6 (s, *para*-C), 127.6 (s, *ortho*-C), 129.6 (s, *meta*-C), 131.2 (d,  $^3J_{\text{PC}} = 13$  Hz, *meta*-C ( $\text{PPh}_3$ )), 134.3 (d,  $^2J_{\text{PC}} = 10$  Hz, *ortho*-C ( $\text{PPh}_3$ )), 135.9 (d,  $^4J_{\text{PC}} = 3$  Hz, *para*-C ( $\text{PPh}_3$ )), 161.6 (s, *ipso*-C).  $^{31}\text{P}$  NMR (121 MHz, PhCl)  $\delta$  23.4 (s). ESI-MS (+ve detection) 689.2124  $m/z$  [ $\text{M}]^+$ , 335.1563  $m/z$  [ $\text{HO}(\text{C}_4\text{H}_8)\text{PPh}_3]^+$ .

**Synthesis of  $[\text{Cp}_2\text{Zr}(\text{THF})\text{OMes}][\text{B}(\text{C}_6\text{F}_5)_4]$  (**1-THF**).** In a glovebox, THF (0.25 mL) was added dropwise to a stirred chlorobenzene (1 mL) solution of **3** (40 mg, 0.4 mmol), resulting in a yellow solution. The product was isolated via precipitation into a large volume (25 mL) of rapidly stirred hexane. The resulting pale yellow powder was washed with pentane ( $3 \times 5$  mL) and dried *in vacuo* (37 mg, 86%). Crystals of **1-THF** suitable for analysis by single crystal X-ray diffraction were obtained by layering a chlorobenzene solution with pentane (7 days).

$^1\text{H}$  NMR (500 MHz,  $d_5$ -PhBr)  $\delta$  1.69 (4H, br s, THF (C3, C4)), 1.84 (6H, s, *ortho*- $\text{CH}_3$ ), 2.21 (3H, s, *para*- $\text{CH}_3$ ), 3.67 (4H, br s, THF (C2, C5)), 6.03 (10H, s, Cp), 6.76 (2H, s, Ar–H).  $^{13}\text{C}$  NMR (125 MHz,  $d_5$ -PhBr)  $\delta$  17.9 (s, *ortho*- $\text{CH}_3$ ), 20.7 (s, *para*- $\text{CH}_3$ ), 25.9 (br s, THF (C3, C4)), 77.8 (br s, THF (C2, C5)), 116.4 (s, Cp), 123.4 (s, *ortho*-C), 129.8 (s, *meta*-C), 160.9 (s, *ipso*-C). NB: All other peaks were obscured by the PhBr solvent.

**Reactivity of  $[\text{Cp}^*_2\text{ZrOMes}][\text{B}(\text{C}_6\text{F}_5)_4]/\text{PR}_3$  (**2a–e**).** In a glovebox, **2** (20 mg, 0.02 mmol) and an equimolar amount of the corresponding phosphine (**a** =  $\text{PCy}_3$  (4.7 mg), **b** =  $\text{PET}_3$  (2.0 mg), **c** =  $\text{PPh}_3$  (4.5 mg), **d** =  $\text{PMes}_3$  (6.6 mg), **e** =  $\text{P}(\text{C}_6\text{F}_5)_3$  (9.0 mg)) were weighed out and dissolved in PhCl (0.7 mL) before transferring to an NMR tube fitted with a J. Young valve. The resulting solution was treated with five drops of THF and a slight lightening of the yellow color observed. The  $^{31}\text{P}$  NMR spectrum of the solution indicated full conversion to free phosphine in all cases caused by its displacement by the THF moiety. When the reaction was deemed complete by  $^{31}\text{P}$  NMR spectroscopy, the product was isolated by precipitation into rapidly stirred hexane, washed with pentane ( $3 \times 5$  mL), and dried *in vacuo*.

**Compound 10.** Yield = 13 mg, 51%.  $^1\text{H}$  NMR (500 MHz,  $d_8$ -THF)  $\delta$  1.40–1.82 (30H, m,  $\text{PCy}_3$ ), 1.91 (2H, m,  $\beta$ - $\text{CH}_2$ ), 2.31 (2H, m,  $\delta$ - $\text{CH}_2$ ), 1.91 (30H, s,  $\text{Cp}^*$ ), 2.04 (3H, s, *ortho*- $\text{CH}_3$ ), 2.12 (3H, s, *ortho*- $\text{CH}_3$ ), 2.18 (3H, s, *para*- $\text{CH}_3$ ), 2.31 (2H, m,  $\gamma$ - $\text{CH}_2$ ), 4.27 (2H, m,  $\alpha$ - $\text{CH}_2$ ), 6.55 (1H, s, Ar–H), 6.64 (1H, s, Ar–H).  $^{13}\text{C}$  NMR (125 MHz,  $d_8$ -THF):  $\delta$  11.8 (s,  $\text{Cp}^*$ -Me), 16.3 (d,  $^1J_{\text{PC}} = 43$  Hz,  $\delta$ - $\text{CH}_2$ ), 18.7 (s, *para*- $\text{CH}_3$ ), 19.9 (s, *ortho*- $\text{CH}_3$ ), 20.1 (d,  $^2J_{\text{PC}} = 5$  Hz,  $\gamma$ - $\text{CH}_2$ ), 20.8 (s, *ortho*- $\text{CH}_3$ ), 26.4 (s, *para*-C ( $\text{PCy}_3$ )), 27.5 (d,  $^3J_{\text{PC}} = 13$  Hz, *meta*-C ( $\text{PCy}_3$ )), 27.8 (d,  $^2J_{\text{PC}} = 4$  Hz, *ortho*-C ( $\text{PCy}_3$ )), 30.8 (d,  $^1J_{\text{PC}} = 43$  Hz, *ipso*-C ( $\text{PCy}_3$ )), 38.2 (d,  $^3J_{\text{PC}} = 14$  Hz,  $\beta$ - $\text{CH}_2$ ), 70.8 (s,  $\alpha$ - $\text{CH}_2$ ), 121.3 (s,  $\text{Cp}^*$ ), 124.6 (s, *para*-C), 125.9 and 126.3 (s, *ortho*-C), 129.5 and 129.8 (s, *meta*-C), 158.0 (*ipso*-C).  $^{31}\text{P}$  NMR (121 MHz, PhCl)  $\delta$  33.9 (s). ESI-MS (+ve detection) 847.5089  $m/z$  [ $\text{M}]^+$ .

**Compound 11.** Yield = 18 mg, 78%.  $^1\text{H}$  NMR (500 MHz,  $d_8$ -THF)  $\delta$  1.29 (9H, dt,  $^3J_{\text{PH}} = 18$  Hz,  $^3J_{\text{HH}} = 7$  Hz,  $\text{CH}_3(\text{PEt}_3)$ ), 1.56 (2H, m,  $\delta$ - $\text{CH}_2$ ), 1.89 (2H, m,  $\beta$ - $\text{CH}_2$ ), 1.91 (30H, s,  $\text{Cp}^*$ ), 2.04 (3H, s, *ortho*- $\text{CH}_3$ ), 2.12 (3H, s, *ortho*- $\text{CH}_3$ ), 2.18 (3H, s, *para*- $\text{CH}_3$ ), 2.24–2.32 (8H, m,  $\gamma$ - $\text{CH}_2$  and  $\text{CH}_2(\text{PEt}_3)$ ), 4.27 (2H, m,  $\alpha$ - $\text{CH}_2$ ), 6.55 (1H, s, Ar–H), 6.64 (1H, s, Ar–H).  $^{13}\text{C}$  NMR (125 MHz,  $d_8$ -THF)  $\delta$  5.62 (d,  $^2J_{\text{PC}} = 5$  Hz,  $\text{CH}_3(\text{PEt}_3)$ ), 11.8 (s,  $\text{Cp}^*$ -Me), 12.1 (d,  $^1J_{\text{PC}} = 49$  Hz,  $\text{CH}_2(\text{PEt}_3)$ ), 18.4 (d,  $^1J_{\text{PC}} = 47$  Hz,  $\delta$ - $\text{CH}_2$ ), 18.7 (d,  $^2J_{\text{PC}} = 4$  Hz,  $\gamma$ - $\text{CH}_2$ ), 18.7 (s, *para*- $\text{CH}_3$ ), 19.9 (s, *ortho*- $\text{CH}_3$ ), 20.8 (s, *ortho*- $\text{CH}_3$ ), 37.6 (d,  $^3J_{\text{PC}} = 14$  Hz,  $\beta$ - $\text{CH}_2$ ), 70.8 (s,  $\alpha$ - $\text{CH}_2$ ), 121.3 (s,  $\text{Cp}^*$ ), 124.6 (s, *para*-C), 125.9 and 126.3 (s, *ortho*-C), 129.5 and 129.8 (s, *meta*-C), 158.0 (*ipso*-C).  $^{31}\text{P}$  NMR (121 MHz, PhCl)  $\delta$  36.8 (s). ESI-MS (+ve detection) 685.3691  $m/z$  [ $\text{M}]^+$ , 191.1540 [ $\text{HO}(\text{C}_4\text{H}_8)\text{PEt}_3]^+$ .

**Compound 12.** Yield = 14 mg, 55%.  $^1\text{H}$  NMR (500 MHz,  $d_5$ -PhBr).  $\delta$  1.78 (2H, m,  $\delta$ - $\text{CH}_2$ ), 1.87 (30H, s,  $\text{Cp}^*$ ), 1.91 (2H, m,  $\beta$ - $\text{CH}_2$ ), 2.01 (3H, s, *ortho*- $\text{CH}_3$ ), 2.05 (3H, s, *ortho*- $\text{CH}_3$ ), 2.17 (3H, s, *para*- $\text{CH}_3$ ), 3.43 (2H, m,  $\gamma$ - $\text{CH}_2$ ), 4.21 (2H, m,  $\alpha$ - $\text{CH}_2$ ), 6.53 (1H, s,



Ar–H), 6.63 (1H, s, Ar–H), 7.72–7.93 (15H, m, PPh<sub>3</sub>). <sup>13</sup>C NMR (125 MHz, *d*<sub>5</sub>-PhBr) δ 11.7 (s, Cp\*), 11.8 (d, <sup>1</sup>J<sub>PC</sub> = 50 Hz, δ-CH<sub>2</sub>), 18.7 (s, *para*-CH<sub>3</sub>), 19.9 (s, *ortho*-CH<sub>3</sub>), 20.8 (s, *ortho*-CH<sub>3</sub>), 22.9 (d, <sup>2</sup>J<sub>PC</sub> = 4 Hz, γ-CH<sub>2</sub>), 37.6 (d, <sup>3</sup>J<sub>PC</sub> = 15 Hz, β-CH<sub>2</sub>), 70.7 (s, α-CH<sub>2</sub>), 121.3 (s, Cp\*), 128.7 and 129.5 (s, *meta*-C), 129.6 (d, <sup>1</sup>J<sub>PH</sub> = 38 Hz, *ipso*-C (PPh<sub>3</sub>)), 131.5 (d, <sup>3</sup>J<sub>PC</sub> = 11 Hz, *meta*-C (PPh<sub>3</sub>)), 134.7 (d, <sup>4</sup>J<sub>PC</sub> = 4 Hz, *para*-C (PPh<sub>3</sub>)), 157.9 (s, *ipso*-C)

Ortho-C peak for the triphenylphosphine is obscured by the solvent. <sup>31</sup>P NMR (121 MHz, PhCl) δ 22.2 (s). ESI-MS (+ve detection) 829.3684 *m/z* [M]<sup>+</sup>, 335.1563 *m/z* [HO(C<sub>4</sub>H<sub>8</sub>)PPh<sub>3</sub>]<sup>+</sup>.

**Synthesis of [Cp\*<sub>2</sub>Zr(THF)OMes][B(C<sub>6</sub>F<sub>5</sub>)<sub>4</sub>]/PR<sub>3</sub> (2-THF).** In a glovebox, THF (0.25 mL) was added dropwise to a stirred chlorobenzene (1 mL) solution of **2** (119 mg, 0.1 mmol), resulting in a yellow solution. The product was isolated via precipitation into a large volume (25 mL) of rapidly stirred hexane. The resulting pale yellow powder was washed with pentane (3 × 5 mL) and dried in vacuo (90 mg, 71%). Crystals of 2-THF suitable for analysis by single crystal X-ray diffraction were obtained by layering a chlorobenzene solution with pentane (7 days).

<sup>1</sup>H NMR (500 MHz, *d*<sub>5</sub>-PhBr) δ 1.59 (4H, s, THF (C3, C4)), 1.61 (30H, s, Cp\*), 1.79 (3H, s, *ortho*-CH<sub>3</sub>), 1.88 (3H, s, *ortho*-CH<sub>3</sub>), 2.19 (3H, s, *para*-CH<sub>3</sub>), 3.55 (4H, s, THF (C2, C5)), 6.03 (1H, s, Ar–H), 6.77 (1H, s, Ar–H). <sup>13</sup>C NMR (125 MHz, *d*<sub>5</sub>-PhBr) δ 10.2 (s, Cp\*–Me), 17.0 (s, *ortho*-CH<sub>3</sub>), 18.3 (s, *ortho*-CH<sub>3</sub>), 20.1 (s, *para*-CH<sub>3</sub>), 25.0 (s, THF (C3, C4)), 67.9 (s, THF (C2, C5)), 122.0 (s, Cp\*), 129.4 (s, *meta*-C), 154.8 (s, *ipso*-C). NB: Remaining peaks in <sup>13</sup>C NMR are obscured by the PhBr solvent.

**4.8. Reaction of Pairs with Phenylacetylene (PhCCH).** **Reactivity of [Cp\*<sub>2</sub>ZrOMes][B(C<sub>6</sub>F<sub>5</sub>)<sub>4</sub>]/PR<sub>3</sub> (1a–e).** In a glovebox, **1** (30 mg, 0.028 mmol) and an equimolar amount of the corresponding phosphine (0.028 mmol, **a** = PCy<sub>3</sub> (8.1 mg), **b** = PEt<sub>3</sub> (3.4 mg), **c** = PPh<sub>3</sub> (7.6 mg), **d** = PMes<sub>3</sub> (11.3 mg), **e** = P(C<sub>6</sub>F<sub>5</sub>)<sub>3</sub> (15.4 mg)) were weighed out and dissolved in PhCl (0.7 mL) before transferring to an NMR tube fitted with a J. Young valve. Excess phenylacetylene (5 drops) was subsequently added, and in the case of **1a–d** an instantaneous lightening of the yellow color was observed. The progress of the reactions was monitored by <sup>31</sup>P NMR spectroscopy. Collected spectral data is detailed below:

**1a.** Reaction complete in <1 min. Mixture of products could not be sufficiently separated to allow further characterization. <sup>31</sup>P NMR (121 MHz, PhCl) δ 33.2 (d, <sup>1</sup>J<sub>PH</sub> = 430 Hz, H-PCy<sub>3</sub>). ESI-MS (+ve detection) 281.2 *m/z* [HPCy<sub>3</sub>]<sup>+</sup>.

**1b.** Reaction complete in 16 h. Mixture of products could not be sufficiently separated to allow further characterization. <sup>31</sup>P NMR (121 MHz, PhCl) δ 25.5 (m, **1b**-PhCCH), 30.3 (m, **1b**-PhCCH). Proposed to be the two possible isomers of **1b**-PhCCH. ESI-MS (+ve detection) 575.2 *m/z* [**1b**-PhCCH], 119.1 [HPet<sub>3</sub>]<sup>+</sup>.

**1c.** The reaction was seen to be complete after <1 min, and compound **13** was isolated in a glovebox by precipitation into rapidly stirred hexane (20 mL) and washed with pentane (3 × 5 mL) before drying in vacuo (27.3 mg, 69%). <sup>1</sup>H NMR (500 MHz, *d*<sub>5</sub>-PhBr) δ 1.65 (6H, s, *ortho*-CH<sub>3</sub>), 2.16 (3H, s, *para*-CH<sub>3</sub>), 5.74 (10H, s, Cp), 6.66 (2H, s, Ar–H), 7.04 (2H, d, <sup>3</sup>J<sub>HH</sub> = 7 Hz, *ortho*-H (PhCCH)), 7.22 (2H, t, <sup>3</sup>J<sub>HH</sub> = 7 Hz, *meta*-H (PhCCH)), 7.32 (1H, t, <sup>3</sup>J<sub>HH</sub> = 7 Hz, *para*-H (PhCCH)), 7.25–7.42 (9H, m, *meta/para*-H (PPh<sub>3</sub>)), 7.56 (3H, t, <sup>3</sup>J<sub>HH</sub> = 7 Hz, *para*-H (PPh<sub>3</sub>)), 9.01 (1H, d, <sup>3</sup>J<sub>PH</sub> = 45 Hz, α-H). <sup>13</sup>C NMR (125 MHz, *d*<sub>5</sub>-PhBr) δ 21.4 (s, *ortho*-CH<sub>3</sub>), 23.7 (s, *para*-CH<sub>3</sub>), 115.2 (s, Cp), 122.6 (s, *para*-C), 126.6 (s, *ortho*-C), 132.5 (*meta*-C), 135.1 (s, *ipso*-C (PhCCH)), 137.1 (d, <sup>3</sup>J<sub>PC</sub> = 10 Hz, *meta*-C (PPh<sub>3</sub>)), 137.9 (d, <sup>4</sup>J<sub>PC</sub> = 3 Hz, *para*-C (PPh<sub>3</sub>)), 138.2 (d, <sup>1</sup>J<sub>PH</sub> = 22 Hz, C-PPh<sub>3</sub>), 163.2 (s, *ipso*-C), 212.6 (d, <sup>3</sup>J<sub>PH</sub> = 10 Hz, Zr–C(H)). <sup>31</sup>P NMR (121 MHz, *d*<sub>5</sub>-PhBr) δ 20.1 (s). NB: Remaining peaks in <sup>13</sup>C NMR are obscured by the PhBr solvent. ESI-MS (+ve detection) 719.2015 *m/z* [M]<sup>+</sup>.

**Reactivity of [Cp\*<sub>2</sub>ZrOMes][B(C<sub>6</sub>F<sub>5</sub>)<sub>4</sub>]/PR<sub>3</sub> (2a–e).** In a glovebox, **2** (20 mg, 0.017 mmol) and an equimolar amount of the corresponding phosphine (0.017 mmol, **a** = PCy<sub>3</sub> (4.7 mg), **b** = PEt<sub>3</sub> (2.0 mg), **c** = PPh<sub>3</sub> (4.5 mg), **d** = PMes<sub>3</sub> (6.6 mg), **e** = P(C<sub>6</sub>F<sub>5</sub>)<sub>3</sub> (9.0 mg)) were weighed out and dissolved in PhCl (0.7 mL) before transferring to an NMR tube fitted with a J. Young valve. Excess phenylacetylene (5 drops) was subsequently added, and in the case of

**2a–d** an instantaneous lightening of the yellow color was observed. The progress of the reactions was monitored by <sup>31</sup>P NMR spectroscopy. Collected spectral data is detailed below:

**2a.** Reaction complete in <1 min. Mixture of products could not be sufficiently separated to allow further characterization. <sup>31</sup>P NMR (121 MHz, PhCl) δ 20.1 (s, **2a**-PhCCH, 38%), 33.2 (d, <sup>1</sup>J<sub>PH</sub> = 450 Hz, HPCy<sub>3</sub>, 62%). ESI-MS (+ve detection) 877.4 *m/z* [**2a**-PhCCH], 281.2 *m/z* [HPCy<sub>3</sub>]<sup>+</sup>.

**2b.** Reaction complete in <1 min. Mixture of products could not be sufficiently separated to allow further characterization. <sup>31</sup>P NMR (121 MHz, PhCl) δ 21.7 (d, <sup>1</sup>J<sub>PH</sub> = 450 Hz, HPet<sub>3</sub>, 46%), 26.0 (s, **2b**-PhCCH, 54%). ESI-MS (+ve detection) 715.4 *m/z* [**2b**-PhCCH], 119.1 [HPet<sub>3</sub>]<sup>+</sup>.

**2c.** The reaction was seen to be complete after <1 min, and compound **14** was isolated in a glovebox by precipitation into rapidly stirred hexane (20 mL) and washed with pentane (3 × 5 mL) before drying in vacuo (24.0 mg, 92%). Crystals of **14** suitable for analysis by single crystal X-ray diffraction were obtained by layering a PhCl solution of **14** with pentane (5 days). <sup>1</sup>H NMR (500 MHz, *d*<sub>5</sub>-PhBr) δ 1.59 (30H, s, Cp\*), 1.17 (3H, s, *para*-CH<sub>3</sub>), 2.10 (3H, s, *ortho*-CH<sub>3</sub>), 2.12 (3H, s, *ortho*-CH<sub>3</sub>), 6.40 (2H, s, Ar–H), 7.50–7.76 (15H, m, PPh<sub>3</sub>), 8.36 (1H, d, <sup>3</sup>J<sub>PH</sub> = 45 Hz, α-H). <sup>13</sup>C NMR (125 MHz, *d*<sub>5</sub>-PhBr) δ 15.4 (s, Cp\*), 17.5 (s, *para*-CH<sub>3</sub>), 22.9 and 23.6 (s, *ortho*-CH<sub>3</sub>), 124.8 (Cp\*), 128.1 (s, *para*-C), 131.7 (s, *ortho*-C), 132.5 (s, *meta*-C), 136.5 (d, <sup>3</sup>J<sub>PH</sub> = 14 Hz, *meta*-C (PPh<sub>3</sub>)), 137.6 (d, <sup>4</sup>J<sub>PH</sub> = 4 Hz, *para*-C (PPh<sub>3</sub>)), 158.9 (*ipso*-C), 233.1 (d, <sup>3</sup>J<sub>PH</sub> = 10 Hz, Zr–C(H)). <sup>31</sup>P NMR (121 MHz, *d*<sub>5</sub>-PhBr) δ 17.4 (d, <sup>3</sup>J<sub>PH</sub> = 48 Hz, 14). NB: Remaining peaks in <sup>13</sup>C NMR are obscured by the PhBr solvent. ESI-MS (+ve detection) 859.3598 *m/z* [M]<sup>+</sup>.

**2d.** Reaction complete in <1 min. In situ analysis of the reaction mixture by <sup>31</sup>P NMR spectroscopy showed clean conversion to deprotonation products; however, the zirconium acetylide complex could not be isolated cleanly. <sup>31</sup>P NMR (121 MHz, PhCl) δ 28.7 (d, <sup>1</sup>J<sub>PH</sub> = 476 Hz, [H-PMes<sub>3</sub>]<sup>+</sup>, 100%).

**2e.** No reaction was evident by <sup>31</sup>P NMR spectroscopy.

## ■ ASSOCIATED CONTENT

### Supporting Information

The Supporting Information is available free of charge on the ACS Publications website at DOI: 10.1021/jacs.5b12536.

Additional experimental data: DOSY spectra, NMR spectra, and X-ray diffraction data (PDF)  
Crystallographic data (CIF)

## ■ AUTHOR INFORMATION

### Corresponding Author

\*duncan.wass@bristol.ac.uk

### Notes

The authors declare no competing financial interest.

## ■ ACKNOWLEDGMENTS

O.J.M. would like to acknowledge Dr. Paul Gates and the University of Bristol Mass Spectrometry Service for their assistance and Dr. Craig Butts for his input on the DOSY experiments.

## ■ REFERENCES

- (a) Stephan, D. W.; Erker, G. *Angew. Chem., Int. Ed.* **2015**, *54*, 6400. (b) Stephan, D. W. *J. Am. Chem. Soc.* **2015**, *137*, 10018. (d) Stephan, D. W. *Acc. Chem. Res.* **2015**, *48*, 306.
- (a) Welch, G. C.; Juan, R. R. S.; Masuda, J. D.; Stephan, D. W. *Science* **2006**, *314*, 1124. (b) Wang, X.; Kehr, G.; Daniliuc, C. G.; Erker, G. *J. Am. Chem. Soc.* **2014**, *136*, 3293. (c) Sajid, M.; Kehr, G.; Wiegand, T.; Eckert, H.; Schwickert, C.; Poettgen, R.; Cardenas, A. J. P.; Warren, T. H.; Fröhlich, R.; Daniliuc, C. G.; Erker, G. *J. Am. Chem.*

Soc. **2013**, *135*, 8882–8895. (d) Scott, D. J.; Fuchter, M. J.; Ashley, A. E. *Angew. Chem., Int. Ed.* **2014**, *53*, 10218.

(3) (a) Mömming, C. M.; Otten, E.; Kehr, G.; Fröhlich, R.; Grimme, S.; Stephan, D. W.; Erker, G. *Angew. Chem., Int. Ed.* **2009**, *48*, 6643. (b) Peuser, I.; Neu, R. C.; Zhao, X. X.; Ulrich, M.; Schirmer, B.; Tannert, J. A.; Kehr, G.; Fröhlich, R.; Grimme, S.; Erker, G.; Stephan, D. W. *Chem. - Eur. J.* **2011**, *17*, 9640. (c) Harhausen, M.; Fröhlich, R.; Kehr, G.; Erker, G. *Organometallics* **2012**, *31*, 2801. (d) Bertini, F.; Lyaskovskyy, V.; Timmer, B.; de Kanter, F.; Lutz, M.; Ehlers, A.; Slootweg, J.; Lammertsma, K. *J. Am. Chem. Soc.* **2012**, *134*, 201.

(4) (a) Rosorius, C.; Kehr, G.; Fröhlich, R.; Grimme, S.; Erker, G. *Organometallics* **2011**, *30*, 4211. (b) Liedtke, R.; Fröhlich, R.; Kehr, G.; Erker, G. *Organometallics* **2011**, *30*, 5222. (c) Rosorius, C.; Daniliuc, C. G.; Fröhlich, R.; Kehr, G.; Erker, G. *J. Organomet. Chem.* **2013**, *744*, 149.

(5) (a) Birkmann, B.; Voss, T.; Geier, S. J.; Ullrich, M.; Kehr, G.; Erker, G.; Stephan, D. W. *Organometallics* **2010**, *29*, 5310. (b) Welch, G. W.; Masuda, J. D.; Stephan, D. W. *Inorg. Chem.* **2006**, *45*, 478.

(6) (a) Welch, G. C.; Stephan, D. W. *J. Am. Chem. Soc.* **2007**, *129*, 1880. (b) Spies, P.; Erker, G.; Bergander, K.; Fröhlich, R.; Grimme, S.; Stephan, D. W. *Chem. Commun.* **2007**, 5072. (c) Mömming, C. M.; Otten, E.; Kehr, G.; Fröhlich, R.; Grimme, S.; Stephan, D. W.; Erker, G. *Angew. Chem., Int. Ed.* **2009**, *48*, 6643.

(7) (a) Ménard, G.; Stephan, D. W. *J. Am. Chem. Soc.* **2010**, *132*, 1796. (b) Appelt, C.; Westenberg, H.; Bertini, F.; Ehlers, A. W.; Slootweg, J. C.; Lammertsma, K.; Uhl, W. *Angew. Chem., Int. Ed.* **2011**, *50*, 3925. (c) Roters, S.; Appelt, C.; Westenberg, H.; Hepp, A.; Slootweg, J.; Lammertsma, K.; Uhl, W. *Dalton Trans.* **2012**, *41*, 9033. (d) Boudreau, J.; Courtemanche, M. A.; Fontaine, F. G. *Chem. Commun.* **2011**, *47*, 11131.

(8) (a) Schäfer, A.; Reissmann, M.; Schäfer, A.; Saak, W.; Haase, D.; Müller, T. *Angew. Chem., Int. Ed.* **2011**, *50*, 12636. (b) Reißmann, M.; Schäfer, A.; Jung, S.; Müller, T. *Organometallics* **2013**, *32*, 6736. (c) Herrington, T. J.; Thom, A. J. W.; White, A. J. P.; Ashley, A. E. *Chem. Commun.* **2012**, *41*, 9019. (d) Herrington, T. J.; Ward, B.; Doyle, L. R.; McDermott, J.; White, A. J. P.; Hunt, P. A.; Ashley, A. E. *Chem. Commun.* **2014**, *50*, 12753. (e) Scott, D. J.; Fuchter, M. J.; Ashley, A. E. *Angew. Chem., Int. Ed.* **2014**, *53*, 10218. (f) Scott, D. J.; Simmons, T. R.; Lawrence, E. J.; Wildgoose, G. G.; Fuchter, M. J.; Ashley, A. E. *ACS Catal.* **2015**, *5*, 5540. (g) Erős, G.; Mehdi, H.; Pápai, I.; Rokob, T. A.; Király, P.; Tárkányi, G.; Soós, T. *Angew. Chem., Int. Ed.* **2010**, *49*, 6559. (h) Gyömöre, A.; Bakos, M.; Földes, T.; Pápai, I.; Domján, A.; Soós, T. *ACS Catal.* **2015**, *5*, 5366.

(9) Flynn, S. R.; Wass, D. F. *ACS Catal.* **2013**, *3*, 2574.

(10) Dehydrocoupling of amine-boranes has been achieved stoichiometrically with main group systems, but never in a catalytic sense. (a) Miller, A. J. M.; Bercaw, J. E. *Chem. Commun.* **2010**, *46*, 1709. (b) Whittell, G. R.; Balmond, E. I.; Robertson, A. P. M.; Patra, S. K.; Haddow, M. F.; Manners, I. *Eur. J. Inorg. Chem.* **2010**, 3967. A single example of catalytic dehydrogenation has been reported however requires melt conditions Appelt, C.; Slootweg, J. C.; Lammertsma, K.; Uhl, W. *Angew. Chem., Int. Ed.* **2013**, *52*, 4256. In contrast, catalytic dehydrogenation of amine-boranes is very well-established for transition metal systems: see Leitao, E. M.; Jurca, T.; Manners, I. *Nat. Chem.* **2013**, *5*, 817 and references therein.

(11) (a) Chapman, A. M.; Haddow, M. F.; Wass, D. F. *J. Am. Chem. Soc.* **2011**, *133*, 8826. (b) Chapman, A. M.; Haddow, M. F.; Wass, D. F. *J. Am. Chem. Soc.* **2011**, *133*, 18463. (c) Chapman, A. M.; Wass, D. F. *Dalton Trans.* **2012**, *41*, 9067. (d) Chapman, A. M.; Haddow, M. F.; Wass, D. F. *Eur. J. Inorg. Chem.* **2012**, *2012*, 1546.

(12) (a) Xu, X.; Fröhlich, R.; Daniliuc, C. G.; Kehr, G.; Erker, G. *Chem. Commun.* **2012**, *48*, 6109. (b) Xu, X.; Kehr, G.; Daniliuc, C. G.; Erker, G. *J. Am. Chem. Soc.* **2013**, *135*, 6465.

(13) (a) Neu, R. C.; Otten, E.; Lough, A.; Stephan, D. W. *Chem. Sci.* **2011**, *2*, 170. (b) Xu, X.; Kehr, G.; Daniliuc, Erker, G. *Organometallics* **2013**, *32*, 7306. (c) Frömel, S.; Kehr, G.; Fröhlich, R.; Daniliuc, C. G.; Erker, G. *Dalton Trans.* **2013**, *42*, 14531.

(14) Nishihara, Y.; Aoyagi, K.; Hara, R.; Suzuki, N.; Takahashi, T. *Inorg. Chim. Acta* **1996**, *252*, 91.

(15) Stapleton, R. A.; Galan, B. R.; Collins, S.; Simons, R. S.; Garrison, J. C.; Youngs, W. J. *J. Am. Chem. Soc.* **2003**, *125*, 9246.

(16) Tolman, C. A. *Chem. Rev.* **1977**, *77*, 313.

(17) Rocchigiani, L.; Ciancaleoni, G.; Zuccaccia, C.; Macchioni, A. *J. Am. Chem. Soc.* **2014**, *136*, 112.

(18) For further details on the experimental conditions employed, see the [Supporting Information](#).

(19) Attempts to isolate **1a**-CO<sub>2</sub>, **1b**-CO<sub>2</sub>, **2a**-CO<sub>2</sub>, and **2b**-CO<sub>2</sub> in an argon atmosphere resulted in decomposition to form [HPR<sub>3</sub>][B(C<sub>6</sub>F<sub>5</sub>)<sub>4</sub>] and an as yet unidentified zirconium containing species.

(20) (a) Borkowsky, S. L.; Jordan, R. F.; Hinch, G. D. *Organometallics* **1991**, *10*, 1268. (b) Breen, B.; Stephan, D. W. *Inorg. Chem.* **1992**, *31*, 4019.

(21) Intermolecular FLPs containing a transition metal have also been reported where the transition metal is purely present as an auxiliary and not as the Lewis acid. See Boone, M. P.; Stephan, D. W. *Chem. - Eur. J.* **2014**, *20*, 3333.

(22) (a) Vatamanu, M. *Organometallics* **2014**, *33*, 3683. (b) Couturier, S.; Gautheron, B. J. *J. Organomet. Chem.* **1978**, *157*, 61.

(23) Pangborn, A. B.; Giardello, M. A.; Grubbs, R. H.; Rosen, R. K.; Timmers, F. J. *Organometallics* **1996**, *15*, 1518.

(24) Nilsson, M. J. *Magn. Reson.* **2009**, *200*, 296–302.